Research Article

A nexus of miR-1271, PAX4 and ALK/RYK influences the cytoskeletal architectures in Alzheimer's Disease and Type 2 Diabetes

Piyali Majumder[1], Kaushik Chanda[1], Debajyoti Das[2], Brijesh Kumar Singh[3], Partha Chakrabarti[2], Nihar Ranjan Jana[4] and ⓘDebashis Mukhopadhyay[1]

[1]Biophysics and Structural Genomics Division, Saha Institute of Nuclear Physics, HBNI, Block-AF, Sector-1, Bidhannagar, Kolkata, West Bengal 700064, India; [2]Cell Biology and Physiology Division, Indian Institute of Chemical Biology, 4 Raja S.C. Mullick Road, Kolkata, West Bengal 700032, India; [3]Cellular and Molecular Neuroscience Laboratory, National Brain Research Centre, Manesar, Gurgaon 122 050, India; [4]India and School of Bioscience, Indian Institute of Technology, Kharagpur, India

Correspondence: Debashis Mukhopadhyay (debashis.mukhopadhyay@saha.ac.in)

Alzheimer's Disease (AD) and Type 2 Diabetes (T2D) share a common hallmark of insulin resistance. Reportedly, two non-canonical Receptor Tyrosine Kinases (RTKs), ALK and RYK, both targets of the same micro RNA miR-1271, exhibit significant and consistent functional down-regulation in *post-mortem* AD and T2D tissues. Incidentally, both have Grb2 as a common downstream adapter and NOX4 as a common ROS producing factor. Here we show that Grb2 and NOX4 play critical roles in reducing the severity of both the diseases. The study demonstrates that the abundance of Grb2 in degenerative conditions, in conjunction with NOX4, reverse cytoskeletal degradation by counterbalancing the network of small GTPases. PAX4, a transcription factor for both Grb2 and NOX4, emerges as the key link between the common pathways of AD and T2D. Down-regulation of both ALK and RYK through miR-1271, elevates the PAX4 level by reducing its suppressor ARX via Wnt/β-Catenin signaling. For the first time, this study brings together RTKs beyond Insulin Receptor (IR) family, transcription factor PAX4 and both AD and T2D pathologies on a common regulatory platform.

Introduction

Epidemiological studies show that type 2 diabetes (T2D) increases the risk of Alzheimer's Disease (AD) by at least 2-fold, although there are only a few mechanistic models that provide a clear pathophysiological link [1]. PET and MRI studies show marked impairment of glucose and energy metabolism in both T2D and AD [2], amyloidogenesis being a salient feature in both. Reportedly, diabetic mice overexpressing islet amyloid polypeptide (IAPP) develop oligomers and fibrils with more severe diabetic traits, akin to AD mice models overexpressing amyloid precursor protein (APP) [3]. Additionally, traits like insulin resistance, altered amyloid metabolism, synaptic dysfunction, activation of the inflammatory response pathways and impairment of autophagy have been shown as common pathological features in both the diseases [4]. With the understanding that several pathological signals are being shared by AD and T2D, AD has been suggested to be a neuroendocrine disorder that resembles T2D [5].

Insulin receptor (IR), a typical receptor tyrosine kinase (RTK), further links both of them through resistance to insulin and other metabolic imbalances. Our recent study lists the differential activities of several human RTKs in *post-mortem* brain tissues of AD patients and liver tissues of T2D patients and categorizes them into functional and regulatory clusters [6]. In this context, we have further shown that two RTKs, Anaplastic Lymphoma Kinase (ALK) and Receptor-like Tyrosine Kinase (RYK), functionally behave in a similar fashion in both the disease situations [6]. Both ALK and RYK

are involved in the regulation of Wnt/β-Catenin signaling [7–9], which behaves aberrantly in both AD and T2D [10]. In AD, Aβ increases GSK3β activity by inhibiting the canonical Wnt Signaling [11]. GSK3β is one of the kinases that hyperphosphorylate Tau protein, leading to the formation of neurofibrillary tangles of AD [12]. In turn, hyperphosphorylated Tau dissociates from microtubule and leads to the cytoskeleton instability [10–12]. In addition, both isoforms of GSK3 (GSK3α and GSK3β) play crucial roles in the insulin signaling of T2D [13]. Also, the non-canonical Wnt/planar cell polarity (PCP) signaling is correlated with the cytoskeleton stability through Wnt/RYK/Dvl/DAAM1/RhoA pathway [14].

Besides these pathways and signaling modalities, Reactive Oxygen Species (ROS) mediated oxidative stress has also been shown to be a common trigger in both the diseases [15]. A ROS producing NADPH oxidase, NOX4, is constitutively active with its regulatory protein tyrosine kinase substrate (Tsk4/5) with multiple SH3 domains [16] and interacts with Growth factor receptor-bound protein 2 (Grb2) naturally [17,18]. Phosphorylation of Nox4 Tyr-491 after IGF-I stimulation is responsible for Nox4 binding to the SH2 domain of Grb2 [18]. Reportedly in AD *post-mortem* brain, in AD cell models as well as in AD mouse model (APP/PS1 mouse), Grb2 transcript is significantly up-regulated [19]. In AD brain, the NOX4 expression is significantly increased with substantial correlation between its activity and age-dependent increases of Aβ and cognitive dysfunction [20,21]. In T2D, pancreatic β-cell dysfunction is promulgated by NOX4 over-activity and is sufficient to induce insulin resistance [22]. Growing number of evidence suggest that Nox4-derived ROS contributes to oxidative stress during the initial and chronic stages of T2D [23].

A third factor of commonality are the causative oligopeptides like Amylin and Aβ. The role of human Amylin was first observed as early in 1901, when it was described as hyaline deposits in the pancreatic islets of T2D patients [24]. Amylin is a Calcitonin family peptide and it tends to interact with GPCRs of class B [25] in non-disease conditions. However, the interaction pattern of misfolded or aggregated Amylin in disease conditions is still unclear. On the other hand, Aβ oligomers interact with the extracellular domain of Metabotropic glutamate receptors (mGluR5), which is another GPCR of class C [26]. More recently Amylin has emerged as a crucial component in AD pathogenesis. Both Amylin and Aβ interact with each other and lead to the formation of cross-seeded oligomers, where Amylin acts as the seed for Aβ aggregation [27–33].

It would be intuitive to think that the microRNAs, transcription factors (TF) and adapter proteins might stitch these factors together. Chanda et al. [34] had deduced several miRNAs from the bioinformatics analysis of the small RNA sequence data of AD like cell model, where AICD was transiently transfected and Aβ was treated externally in SHSY5Y cells. The analysis showed alteration of the expression of miR-1271 [34] among others, in the AD like situation. Reportedly, miR-1271 is up-regulated in palmitate induced insulin resistance in HepG2 cell lines [35]. In recent times the therapeutic potential of a cell-lineage specific TF, Paired Box Protein 4 (PAX4), is under scanner for T2D treatment [36]. A previous study showed elevated expression of PAX4 in islets derived from T2D donors owing to high circulating blood glucose [37]. PAX4 regulates the development of islets of Langerhans by increasing the β and δ-cells population [38]. Concomitantly, another TF, Aristaless Related Homeobox (ARX), up-regulates the α-cell population while reducing the β and δ-cells proliferation [39]. Furthermore, PAX4 and ARX are not only antagonistic functionally, they negatively regulate the transcriptions of their own genes [39,40]. PAX4 has also been shown to be involved in inducing regenerative capacity in insulin-positive islet cells in mice [36,41]. *PAX4* mutation have been implicated in T2D [42] and its overexpression led to β-cell proliferation and apoptosis reduction [43]. Only very recently *PAX4* has been implicated in denervation [44] and neurodegeneration, especially in Parkinson's disease models [45]. Reportedly, ARX mutation is associated with neurodegenerative and neurodevelopmental disorders through the impairment of the Wnt/β-Catenin signaling pathway [46–48]. Additionally, hippocampal and select cortical neurons in AD manifest phenotypic changes indicative of neurons re-entering cell division cycle [49,50]. Pathological signals trigger the Grb2/SOS/Ras cascade [51] that initiates cell cycle re-entry and proliferation but remains incomplete due to the lack of cell division machinery. Grb2 happens to be an important adapter of the insulin receptor and interestingly, insulin resistance is a noteworthy phenotype common to AD and T2D.

In the backdrop of AD and T2D, the present study, in one hand focuses on the regulation of both Grb2 and NOX4 by TFs like PAX4, and at the same time explores the roles of miRNA regulated non-canonical RTKs. We have investigated the consequences of pathological perturbations in both the diseases, starting from RTK signaling through their downstream effectors with an aim to link them with the culminating cellular event of cytoskeleton stability and its underpinning transcriptional regulation. Specifically, the study for the first time attempts to interpret the effects of contrasting and extraneous signals, akin to AD and T2D that utilize similar signaling gateways to achieve common outcome in two apparently diverse diseases.

Materials and methods

AD and T2D human tissues

AD (NB820-59363) and Non-AD (NB820-59177) post-mortem whole brain lysates and Type 2 Diabetic (NB820-59232) and Non-Diabetic (NB820-59291) post-mortem whole liver lysates were purchased from Novus Biologicals. For statistical reasons, we procured products from different patients with different lot numbers (for patients details see Supplementary Table S1a,b).

Ethics statement

All animal experimentations using AD and T2D mouse models were conducted following the institutional guidelines for the use and care of animals and approved by the Institutional Animal and Ethics Committee of NBRC, Gurgaon (NBRC/IAEC/2012/71) and IICB, Kolkata (IICB/AEC/Meeting/2016/AUG), respectively.

APP/PS1 mice

APP/PS1 or B6C3-Tg (APPswe, PSEN1dE9/) 85Dbo/J mice were obtained from the Jackson Laboratory (U.S.A.) and maintained in the Institutes animal house facility. These transgenic mouse line for AD express human APPswe mutations (K670N and M671L) and exon 9-deleted human presenilin 1(PSEN1dE9) under the control of the mouse prion gene promoter. Animals were provided water and food /ad libitum/. The genotyping was carried out using PCR as described previously [52]. AD mice along with controls at their age of 8 and 12 months were anaesthetised with Xylazine (10 mg/kg body weight) and Ketamine (100 mg/kg body weight) and perfused transcardially with PBS followed by 4%paraformaldehyde (w/v) in PBS. Brains were collected and further placed in 4% paraformaldehyde for 24 h and then treated with 10, 20 and 30% sucrose (in PBS) followed by sectioning in freezing microtome (20 μm thickness). Sections (both control and AD) were placed on the same slides. These APP/PS1 mice were maintained in the animal house facility of NBRC, Gurgaon.

C57BL/6 mice with obesogenic western diet (OWD)

Animal experiments were performed under the approved Institutional Animal Ethics Committee (Approved by CPCSEA, India) protocol. Wild-type male C57BL/6 mice (6–8 weeks old) were kept at ambient temperature ($22 \pm 1°C$) maintaining 12 : 12 h light-dark cycles and fed with standard chow diet (4.3% lipid and 70% carbohydrate) and/ or obesogenic western diet (45% kcal fat, MP Biomedical) for respective experiments. Weight and age-matched male C57BL/6 mice were fed with an obesogenic western diet for up to 24 weeks. These C57BL/6 mice were maintained in the animal house facility of IICB, Kolkata.

We have tested for gradual weight gain and hyperglycemia at each 4 weeks interval. All mice were fasted for 6 h and fasting blood glucose was measured using a calibrated glucometer by taking one drop of blood from the tail tip cut (Supplementary Figure S1).

AD and T2D cell models, cell culture, transfection, plasmids, siRNAs and antibodies

Clones of both Amyloid-β Protein Precursor Intracellular Domain-GFP (AICD-GFP) construct or 'AICD' and Grb2-DsRed construct or 'Grb2' were available in the lab [53–57]. ALK (siRNA ID: s1269; no. 4392420), RYK (siRNA ID: s12390; no. 4390824) and PAX4 (Assay ID s10061, 4392420) siRNAs were purchased from Ambion, life technologies™. Amyloid β (Aβ)-peptide (A980), Sodium Palmitate (P9767) and Insulin (I9278-5ML) were purchased from Sigma–Aldrich. Amylin (ab142398) was purchased from Abcam. Antibodies were purchased from Abcam and CST (see Supplementary Table S2 for details).

Human neuroblastoma (SHSY-5Y) and liver carcinoma (HepG2) cell-lines were obtained from National Cell Science Centre, Pune, India and were cultured in respective media of DMEM-F12 (Gibco) and DMEM (Gibco) supplemented with 10% fetal bovine serum (Gibco) at 37°C in 5% CO_2 atmosphere under humidified condition. Transfection of cells were done using Lipofectamine 2000 (Invitrogen) and as described [19]. For co-transfection, constructs were taken in equal proportions. Human neuroblastoma (SHSY-5Y) were transiently transfected with AICD and were externally treated with 0.5 μM Aβ 1–42 (Sigma A980) for 3 h after transfection and samples were collected after 48 h of addition [58]. An amount of 0.75 mM aqueous Sodium Palmitate (Sigma P9767) along with 1% fatty acid free BSA (Sigma A8806-5G) was added to 24 h serum starved media of HepG2 cells. Aqueous Amylin (Abcam ab142398) was added to the media at a final concentration of 0.5 μM

after 3 h treatment of Palmitate. Samples were then collected after 16 h with or without insulin (Sigma I9278-5ML) (100 nM) shock of 10 min.

Protein from mammalian cell

Phosphate buffer saline (PBS) washed pellet from cell lines were lysed on ice in lysis buffer (1 M Tris–HCl, pH 7.5, 1 N NaCl, 0.5 M EDTA, 1 M NaF, 1 M Na$_3$VO$_4$, 10% SDS, 20 mM PMSF, 10% Triton X-100, 50% glycerol) for 30 min in presence of complete protease inhibitor (Roche Diagnostics) and centrifuged at 13 000**g** for 15 min. Protein concentration was determined by Bradford protein estimation assay. Western blots and quantification were done as per described protocol [19]. Depending on the antibodies specificity and the cross reactivity, multiple antibodies were probed on a single blot.

Fluorescence-activated cell sorting (FACS) and estimation of ROS activity

Palmitate/Amylin treated HepG2 cells were harvested and stained with CM-H$_2$DCFDA (5-(and-6)-chloromethyl-2′,7′ dichlorodihydrofluoresceindiacetate, acetyl ester) according to manufacturer's protocol. The cells were then analyzed for ROS activity by FACS (BD FACS Calibur platform, U.S.A.).

RNA isolation, c-DNA preparations and real time PCR

RNA was isolated from cells by TRIzol Reagent (Invitrogen, U.S.A.) extraction method following manufacturer's protocol which discussed in Majumder et al. 2017 [19]. Real time RT-PCR reaction was carried out using Syber green 2X Universal PCR Master Mix (Applied Biosystems, U.S.A.) in ABI Prism 7500 sequence detection system. The absolute quantification given by the software was in terms of CT values. The relative quantification of target genes was obtained by normalizing with internal control gene (GAPDH gene). Primer sequences and PCR conditions are mentioned in Supplementary Table S3.

Chromatin immuno precipitation (ChIP)

We used High Sensitivity ChIP Kit (ab185913) to perform the ChIP assay and followed manufacturer's protocol. qRT-PCR analysis was done with the purified DNA using primers for *GRB2* and *NOX4* gene, more specifically around the *PAX4* binding sequence. Primer details are given in Supplementary Table S4.

Validation of ALK and RYK double knockdown model

ALK and RYK double knockdown models were established in two cell lines, SHSY-5Y (human neuroblastoma cells) and HepG2 (human liver carcinoma cells). Here ALK and RYK two genes were simultaneously knocked down in cells by using siRNAs against both ALK and RYK compared with cells where two non-targeted (MOCK) siRNAs were simultaneously knocked down. The extent of knockdown was checked by measuring expression levels of both ALK and RYK by western blot in both SHSY-5Y and HepG2 cells.

Statistical and bioinformatics analysis

Unpaired '*t*' test was carried out to compare the means of two experimental groups. The error bar represents standard error [(standard deviation/ $\sqrt{n}$); n = sample size]. To arrive at the statistically significant sample size for each experiment we did power analysis using the *apriori* model [59] as incorporated in the G*power 3.1 [60] software [19].

We used Transfac$^{®}$ MATCH1.0 (http://www.gene-regulation.com/pub/programs.html#match) online search tool to identify the TFs for the Grb2 and NOX4 gene. Additionally, miRDB [61] (http://www.mirdb.org) was used to analyze the targets of miR-1271.

Gene enhancers (genehancer) were identified using genehancer v4.8 database (downloaded from https://genecards.weizmann.ac.il/geneloc/index.shtml) [62].

Results

miRNA 1271 restricts the expressions of ALK/RYK that in turn elevate Grb2/NOX4 levels

We began with estimating the transcriptional and translational levels of Grb2 and NOX4 in both AD and T2D like situations. The expression level of NOX4 was elevated by 1.86 fold (Figure 1A,B; Supplementary Figure S2) in AD *post-mortem* brain as opposed to non-AD control. Grb2 and NOX4's expression levels were higher by
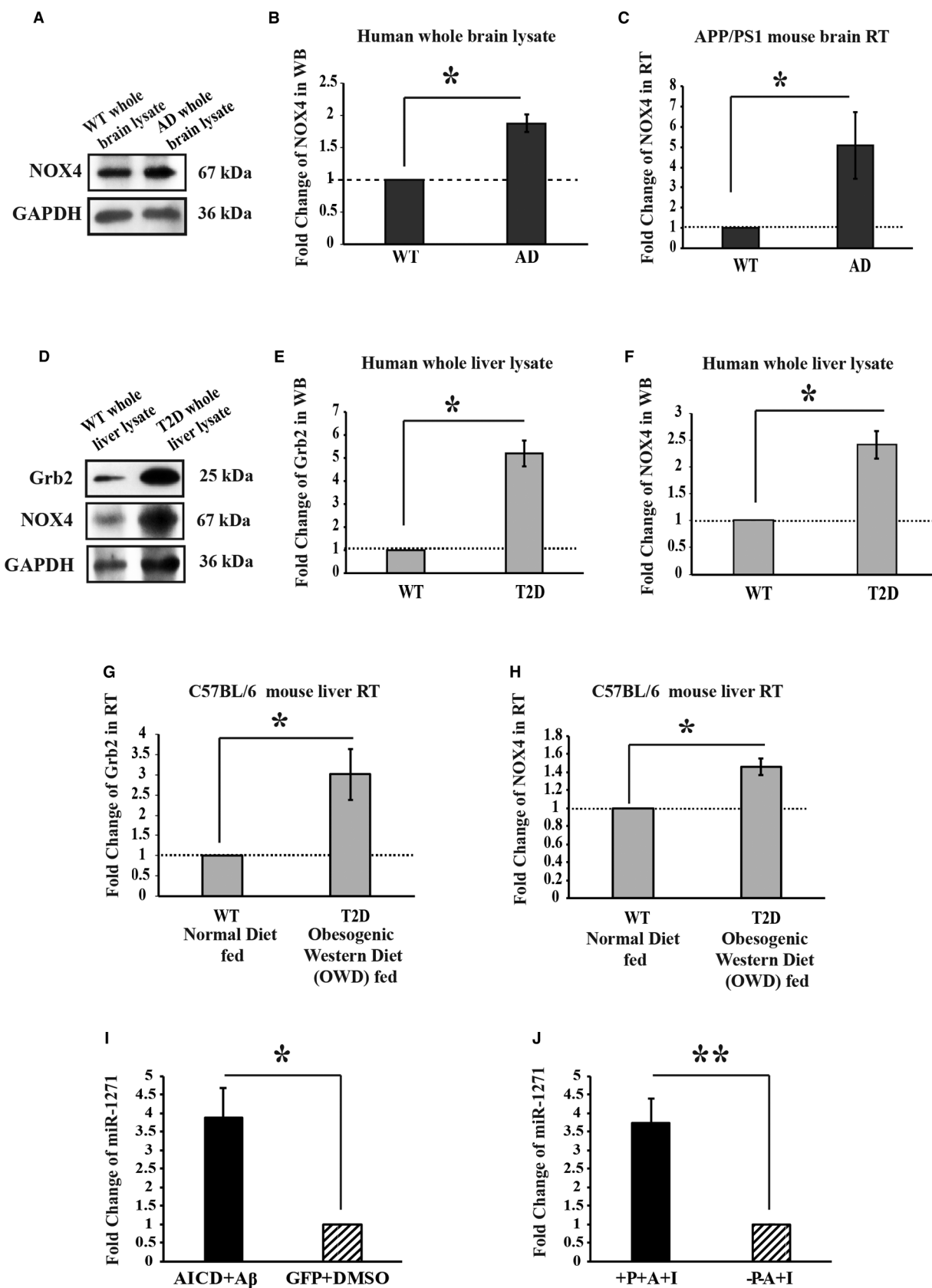
Figure 1. Alteration of expression of Grb2 and NOX4 in clinical, in AD or T2D mimicking mouse.

Part 1 of 2

(**A**) Western blot showing the NOX4 and GAPDH levels in AD whole brain lysate. (**B**) Histogram representing the mean value of optical density of the

Figure 1. Alteration of expression of Grb2 and NOX4 in clinical, in AD or T2D mimicking mouse. Part 2 of 2

bands, normalized against GAPDH. NOX4 was overexpressed by 1.86 fold in AD Brains. (**C**) Shows NOX4 transcript level being up-regulated by 5.06 fold by qRT-PCR of APP/PS1 mouse brain tissue. (**D**) Western blot showing Grb2, NOX4 and GAPDH levels in T2D whole liver lysate. (**E** and **F**) Histograms representing the mean values of Grb2 and NOX4 normalized against GAPDH. Grb2 and NOX4 were overexpressed in T2D liver by 5.27 fold and 2.4 fold, respectively. (**G** and **H**) show qRT-PCR results inT2D mouse model where C57BL/6 mice are maintained in OWD, Grb2 and NOX4 transcript levels are overexpressed by 3.01 fold and 1.45 fold, respectively. (**I** and **J**) the transcript levels of miR-1271 in AD and T2D cell model, respectively. All the statistical information is compiled in Supplementary Table S7.

5.27 and 2.4 folds in human *post-mortem* liver tissue of T2D patients with respect to control, respectively (Figure 1D–F). Similarly, the transcript levels of Grb2 in T2D mice were raised by 3.01 fold (Figure 1G) and that of NOX4 in both AD and T2D mice showed significant up-regulation of 5.06 and 1.45 folds, respectively (Figure 1C,H). Additionally, Grb2 and NOX4 expression levels were up-regulated significantly in T2D mice (Supplementary Figure S3) and cell (Supplementary Figure S4) models.

In SHSY-5Y cells, knockdown of ALK and RYK down-regulated their expression levels by 2.42 (Supplementary Fig. S5A(i),B(i); * $P = 0.0088 < 0.05$; $n = 3$) and 1.2 folds (Supplementary Figure S5A (ii),B(iii); $^\star P = 0.019 < 0.05$; $n = 2$), respectively. In HepG2 cells, knockdown of ALK and RYK reduced the expression levels of ALK by 1.38 fold (Supplementary Figure S5A(iv),B(ii); * $P = 0.0088 < 0.05$; $n = 2$) whereas RYK did not show significant decrease (Supplementary Figure S5A(v),B(iv); N.S.; $P = 0.22 > 0.05$; $n = 2$). We designed double knockdown models for both ALK and RYK genes in SHSY-5Y and HepG2 cells (Supplementary Figure S5). Grb2 protein and transcript levels showed significant up-regulation for double knockdown condition of SHSY-5Y (1.22 fold in protein level, 4.08 fold in transcript level) (Supplementary Fig. S6A,B,F) and HepG2 cell lines (2.34 fold in protein level, 5.9 fold in transcript level), respectively (Supplementary Figure S6A,C,F). Similarly, protein and mRNA expression levels for NOX4 was also elevated significantly for both SHSY-5Y (1.35 fold in protein level 3.02 fold transcript level) (Supplementary Figure S6A,D,G) and HepG2 cell lines (2.62 fold in protein level 4.13 fold transcript level) (Supplementary Figure S6A,E,G). Interestingly, miRNA target analysis using miRDB revealed that both ALK and RYK were prominent target genes for miR-1271 (Supplementary Information S1). This was validated by the qRT-PCR results, which showed significant increase in miR-1271 transcript levels in both AD cell model and T2D cell model (palimitic acid and amylin treated HepG2 cells) by 3.8 and 3.7 folds, respectively (Figure 1I,J). Additionally, the bioinformatics analysis of MIR1271 gene gave us the genehancers using genehancer v4.8 database. The GH05J17641 showed the significantly high score compared with other genehancers and it had 186 transcription binding sites (Supplementary Figure S7). The SP1 transcription factor had the binding site in GH05J17641 genehancer.

PAX4 regulates the transcription of *GRB2* and *NOX4*

To search for the molecular players behind *GRB2* and *NOX4* transcriptional up-regulation, we used Transfac® tool to search upto 10 Kb upstream of both the genes. In case of *GRB2*, 36 probable binding sites for 18 different TFs (Supplementary Table S5) were found, whereas, for *NOX4*, 32 probable binding sites for 16 different TFs (Supplementary Table S6) were noted. Comparing both the results, three (Nkx2-5, Foxd3 and PAX4) top hits were selected among the six common (Nkx2-5, Foxd3, PAX4, CHOP C/EBP, Oct1 and Evi-1) ones. The transcript levels of these three TFs were measured for both AD and T2D cell models (Figure 2A,B) and it was seen that whereas the mRNA levels of *Nkx2-5* were down-regulated, those of *PAX4* and *FOXD3* were up-regulated in both the models.

Specifically, perturbation of PAX4 was most significant and noticeable. PAX4 expression was measured by western blot and was found to be overexpressed in both AD and T2D cell models (Supplementary Figure S8). This was validated with clinical samples of AD and T2D (Figure 2C–E), where PAX4 expression was up-regulated by 1.8 and 2 folds, respectively. Consequences of PAX4 knockdown using Silencer® select *PAX4* siRNA constructing SHSY-5Y and HepG2 (Figure 2F) have been measured. Although non-significant in SHSY-5Y, the transcript level of *GRB2* decreased significantly in HepG2 (Figure 2G) consequently. Additionally, PAX4 knockdown significantly decreased the level of *NOX4* in SHSY-5Y, and in HepG2, the change was insignificant (Figure 2H). We went further to measure the mRNA levels of *Nkx2-5, PAX4* and *FOXD3* in *ALK/RYK* double knockdown cells. qRT-PCR results showed +5.75, +5.84 and +3.13 folds' alterations, respectively, in SHSY-5Y (Figure 3A) and +2.91, +4.8 and +2.46 fold changes, respectively, in HepG2 (Figure 3B). Thus, *ALK/RYK* double knockdown cells
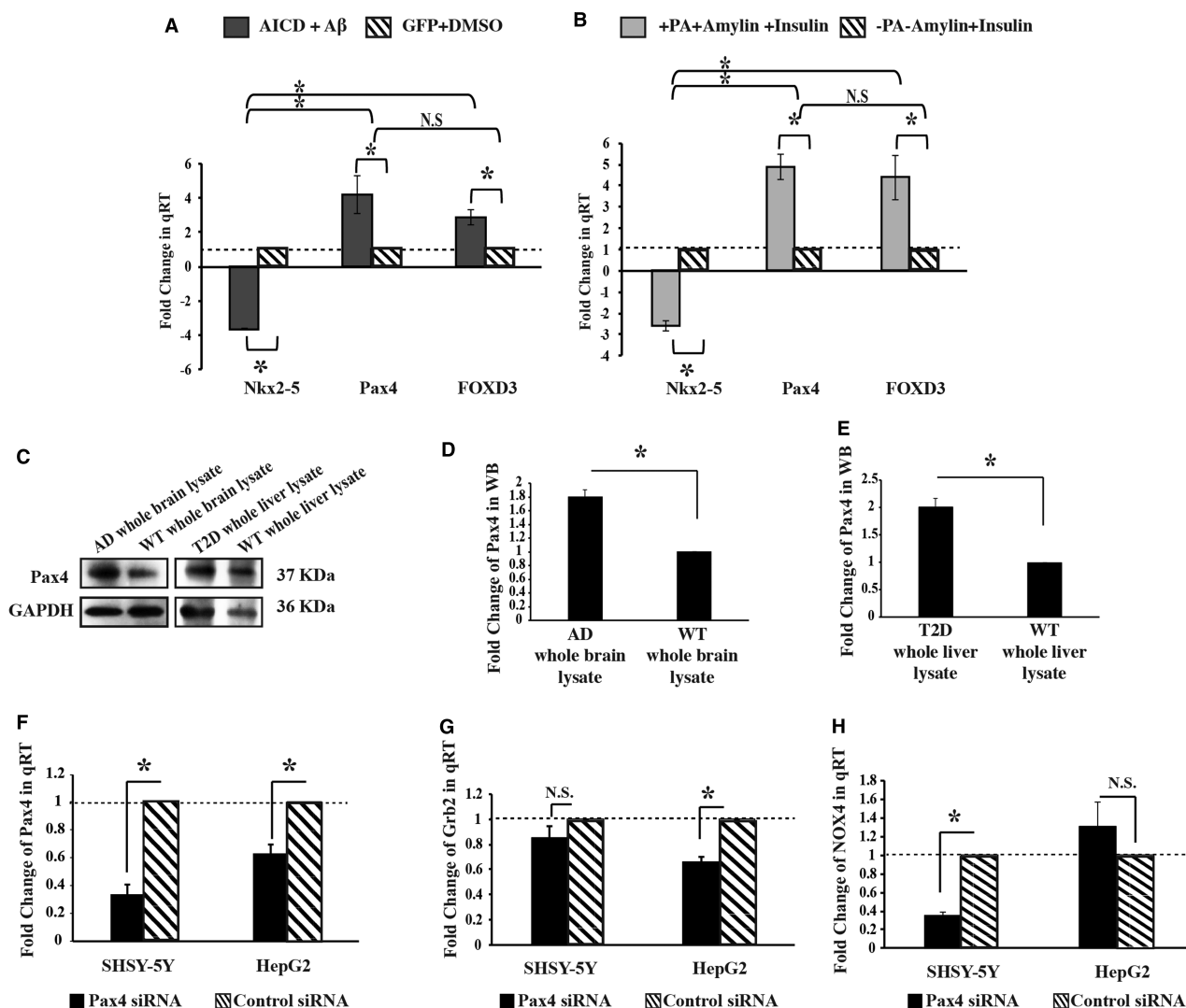
Figure 2. Role of PAX4 in transcription of Grb2 and NOX4.

(**A**) shows the transcript level alterations of −3.6 fold for *Nkx2-5*, +4.19 fold for *PAX4* and +2.89 fold for *FOXD3* in AD (AICD + Aβ) cell models compared with control. Similarly, (**B**) shows the transcript level alterations of −2.59 fold for *Nkx2-5*, +4.88 fold for *PAX4* and +4.39 fold for *FOXD3* in T2D (+PA, +Amylin, +Insulin) cell models compared with controls. (**C**) shows PAX4 protein overexpression by 1.8 and 2.00 folds by Western Blot in (**D**) AD patients' whole brain samples and (**E**) T2D patients' whole liver samples, respectively. The alterations in transcript levels of (**F**) endogenous *PAX4* [in SHSY5Y 2.99 fold and in HepG2 1.58 fold], (**G**) *GRB2* [in SHSY-5Y 1.16 fold and in HepG2 1.52 fold], and (**H**) *NOX4* [in SHSY5Y 2.83 fold and in HepG2 2.3 fold] in PAX4 knockdown situation in SHSY5Y and HepG2 cell lines. All statistical information is compiled in Supplementary Table S7.

resembled AD and T2D cell models in terms of *PAX4* up-regulation. Expectedly, both the double knockdown models showed significant up-regulation of PAX4 protein levels in SHSY-5Y and HepG2 by 1.65 and 1.98 folds, respectively (Figure 3C–E). Furthermore, Chromatin Immuno-precipitation (ChIP) assays confirmed elevated recruitment of PAX4 protein on the *GRB2* and *NOX4* upstream regions. For the AD cell model PAX4 recruitment increased by 27.49 and 5.35 folds (Figure 3F) and in T2D cell model it was elevated by 18.33 and 7.22 folds (Figure 3G), for *GRB2* and *NOX4* genes, respectively.

ARX couples ALK/RYK down-regulation with PAX4 via β-Catenin signaling

In the course of exploring the mechanism behind PAX4 up-regulation in the degenerative diseases, the role of ARX was evident. The significant up-regulation of ARX transcript levels by 3.3 and 3.1 folds in PAX4
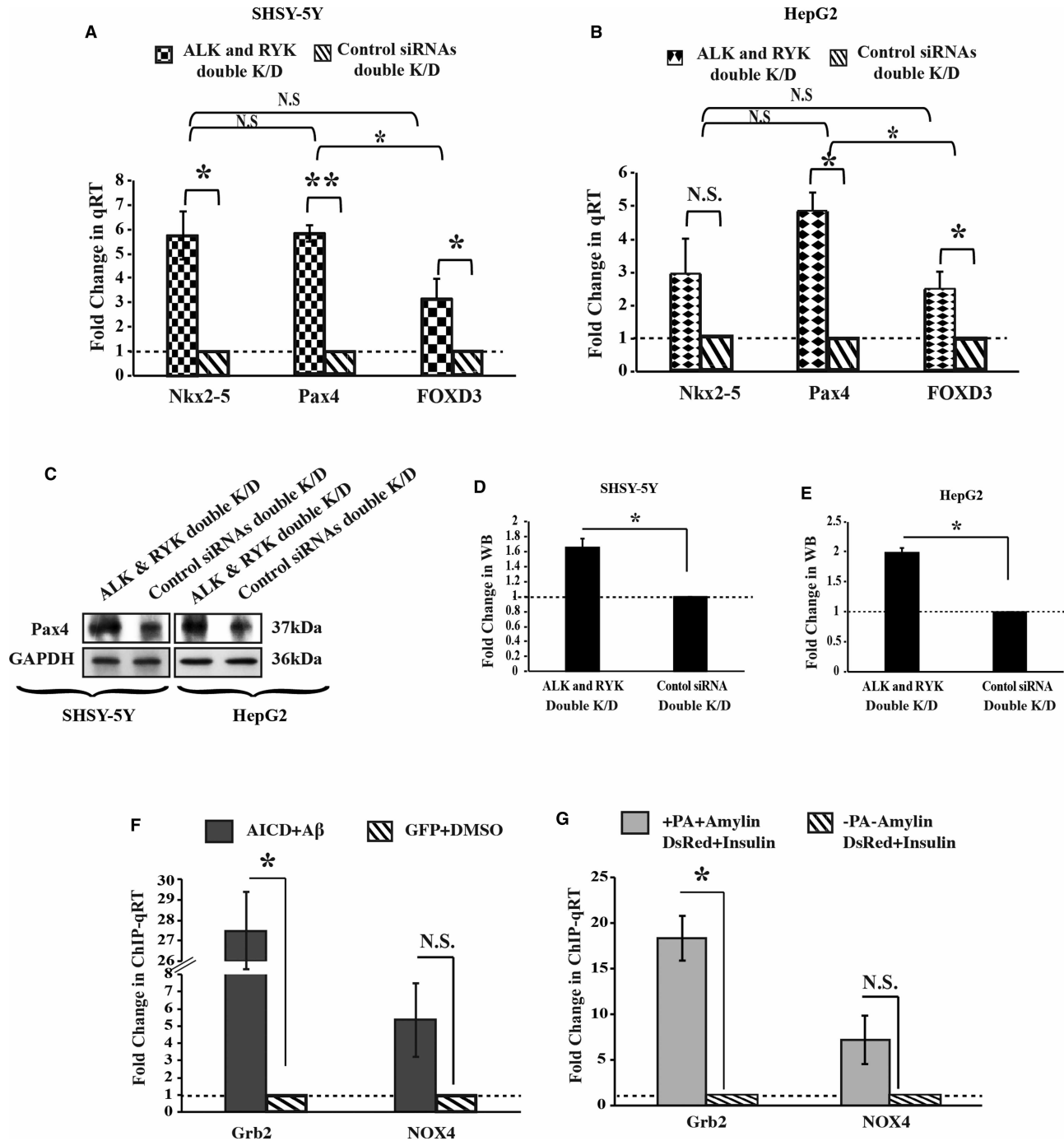
Figure 3. Effect of ALK and RYK double knockdown on PAX4 levels.

The transcript level alterations of *Nkx2-5, PAX4* and *FOXD3* in ALK and RYK double knockdown (K/D) situation in (**A**) SHSY-5Y [+ 5.75 fold for *Nkx2-5*, +5.84 fold for *PAX4* and +3.13 fold for *FOXD3*] and (**B**) HepG2 cell line [+2.91 fold for *Nkx2-5*, +4.81 fold for *PAX4* and +2.46 fold for *FOXD3*]. (**C**) shows the PAX4 protein level alterations by Western Blot in ALK and RYK double knockdown (K/D) model in both SHSY-5Y and HepG2 cell lines. (**D** and **E**) histograms that graphically denotes the up-regulation of endogenous PAX4 levels in double knockdown model in both SHSY-5Y [+1.65 fold] and HepG2 cells [+1.98 folds], respectively. PAX4 binds to the upstream region of Grb2 and NOX4 gene. The ChIP data shows that PAX4 significantly up-regulates *GRB2* expression in both (**F**) AD [+27.49 fold] and (**G**) T2D [+18.33 fold] cell models by binding at its upstream region and acting like an enhancer. In case of *NOX4*, PAX4 fails to significantly up-regulate its expression in both (**F**) AD [+5.35 fold] and (**G**) T2D [+7.22 fold] cell models. All the statistical information is available on Supplementary Table S7.
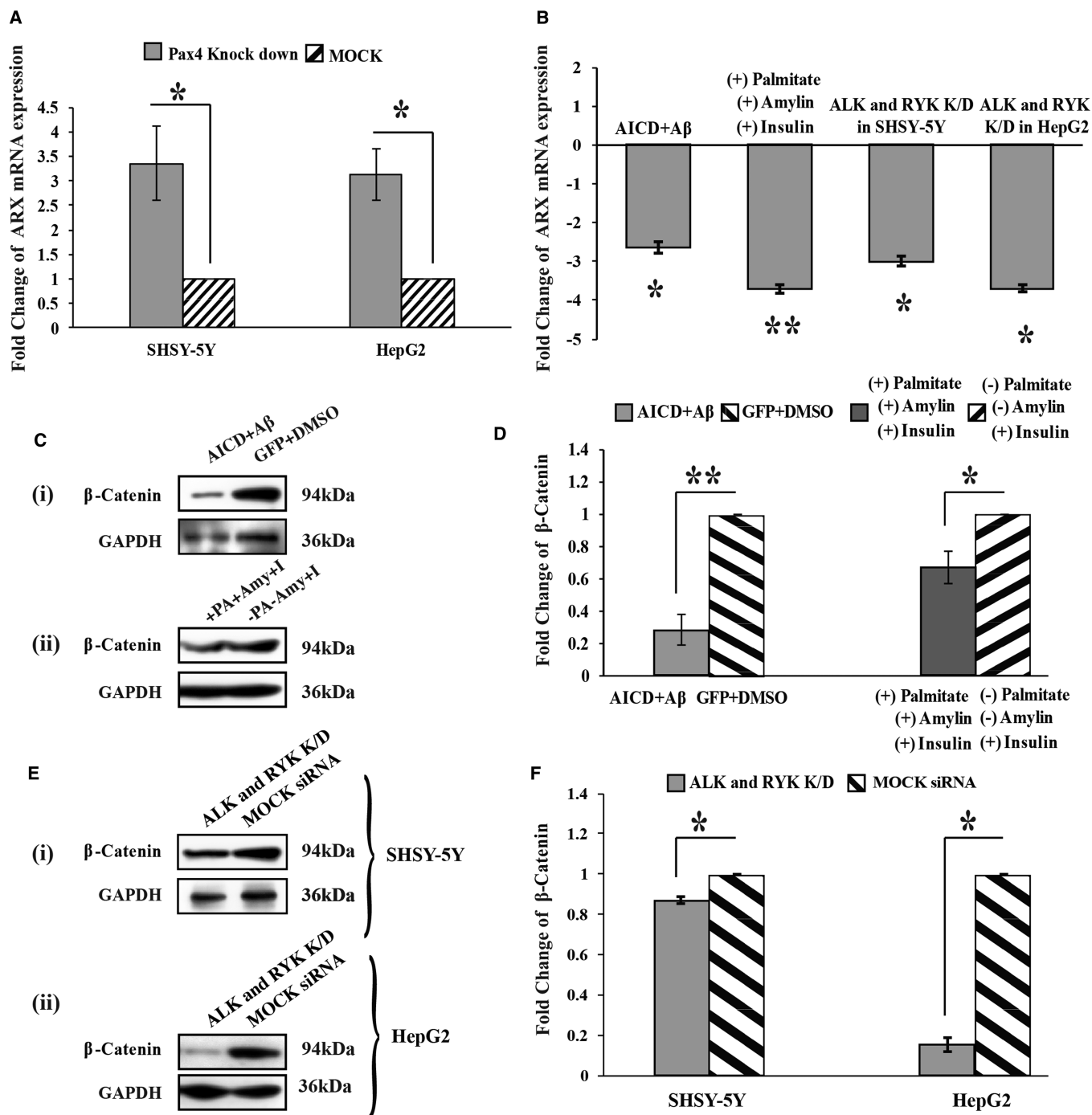
Figure 4. Role of ARX and β-Catenin in AD and T2D cell model and in ALK/RYK double knockdown model.

(**A**) shows that ARX transcript level is being up-regulated in PAX4 knockdown condition by 3.35 and 3.13 fold by qRT-PCR in both SHSY-5Y and HepG2 cells, respectively. (**B**) Shows the down-regulation of ARX transcript levels by 2.6, 3.7, 3 and 3.7 folds in AD (AICD + Aβ) and T2D (+PA, +Amylin, +Insulin) cell models and also in ALK/RYK double knockdown conditions in SHSY-5Y and HepG2 cells, respectively. (**C**) Western blot showing the reduction in β-Catenin expression levels in (**i**) AD and (**ii**) T2D cell model. (**D**) Histogram representing β-Catenin being down-regulated by 3.5 and 1.5 fold in AD and T2D cell models, respectively. (**E** and **F**) shows the down-regulation of β-Catenin expression levels in ALK and RYK double knockdown situation in both (**i**) SHSY-5Y and (**ii**) HepG2 cells by 1.15 and 6.5 folds, respectively. All the statistical information is available in Supplementary Table S7.

knockdown conditions, in both SHSY-5Y and HepG2 cells, established the mutually repressive natures of ARX and PAX4 (Figure 4A). Moreover, the ARX transcript levels were significantly down-regulated by 2.6, 3.7, 3 and 3.7 folds in the AD and T2D cell models and *ALK/RYK* double knockdown in both SHSY-5Y and HepG2 cells, respectively (Figure 4B). Additionally, β-Catenin's role as ARX-regulator was also established by measuring its expression levels. Western blots showed significant down-regulation of β-Catenin by 3.5 and 1.5 folds in AD and T2D cell models, respectively (Figure 4C,D). The *ALK/RYK* double knockdown also showed a significant β-Catenin down-regulation by 1.15 and 6.5 folds in both SHSY-5Y and HepG2 cells, respectively (Figure 4E,F).

Expressions of cytoskeletal proteins change in conjunction with ALK/RYK deactivation

To explore cytoskeletal degradation, the protein and transcript levels of four cytoskeleton proteins (viz., α-Tubulin, Vimentin, α-Smooth muscle actin (α-SMA) and Stathmin1) were compared between the whole liver tissue of T2D patients and non-Diabetic whole liver samples. The relative protein levels were down-regulated by 1.16 fold for α-Tubulin, 1.83 fold for Vimentin, 1.68 fold for α-SMA, and 1.95 fold for Stathmin1, respectively (Figure 5A,B). The transcript levels also showed significant (-5.3 fold α-tubulin; -6.49 fold Vimentin; -2 fold α-SMA and -2.9 fold Stathmin1) down-regulation in T2D mice (Figure 5C). Similarly, in the T2D cell model the relative protein levels were down-regulated by 2.7 fold for α-Tubulin, 1.98 fold for Vimentin, 1.27 fold for α-SMA and 1.97 fold for Stathmin1, respectively (Figure 5D,E). Moreover, to link degeneration with ALK/RYK deactivation, we compared the protein and the transcript levels of α-Tubulin in *ALK/RYK* double knockdown conditions. A significant reduction in protein levels (2.64 and 1.42 folds, respectively) was observed in both SHSY-5Y and HepG2 cell lines (Figure 5F,G). Similarly, transcript levels of α-Tubulin were also down-regulated by 2.3 and 1.5 folds for both SHSY-5Y and HepG2 cell lines, respectively (Figure 5H). In both Palmitate and Amylin treated situations, the percentage recovery of cytoskeletal proteins from disassembly, upon Grb2 overexpression, up-regulated the expressions of α-Tubulin, Vimentin, α-SMA and Sthathmin1 by 98.2%, 84.39%, 508.8% and 62.2%, respectively (Figure 5I).

The signaling pathways also show a reversal of outcome through Grb2–NOX4 interaction

While investigating the pathways that could be responsible for degradation of cytoskeletal proteins, involvement of three small GTPases viz., RhoA, Rac1 and Cdc42 (Figure 6A,B) was observed. Similar to AD situations, under Palmitate and Amylin treated disease inducing conditions, the expression levels of RhoA and Rac1 decreased significantly by 2.13 ($n = 3$) and 1.63 folds ($n = 3$) respectively and the Cdc42 protein levels increased by 64.2% ($n = 3$). Down the line, the significantly reduced Cofilin activity bounced back by 43.2% (Figure 6C,D) upon Grb2 overexpression and Palmitate/Amylin treatment. Besides these, SSH-1's (an activator of Cofilin through dephosphorylation) distal upstream effector NOX4 was overexpressed significantly by 1.31 fold post Palmitate/Amylin treatment, that did reduce significantly by 1.26 fold (Figure 6E,F) upon Grb2 overexpression. Interestingly, Nox4, an interactor of Grb2, was found to be 1.34 fold overexpressed endogenously in T2D cell model but reduced in the presence of Grb2 (Figure 6E,F). We validated the interaction between NOX4 and Grb2 with co-immunoprecipitation (Co-IP) experiment. We pulled down the interacting complex by anti-Grb2 antibody and probed the expression of NOX4 in that complex by immunoblot. The interaction of Grb2 with NOX4 was enhanced 1.35 fold in T2D scenario (Figure 7A,B). Furthermore, the intensity of interaction of NOX4 and Grb2 was checked in T2D mouse liver lysate that increased 2.87 fold in T2D situation compared with the wild type (Figure 7C,D). Besides the reversal, we also measured the ROS activities of Palmitate/Amylin and Palmitate/Amylin/Grb2 by flow cytometry by using CMH2-DCFDA ROS indicator. Although overexpressed Grb2 could significantly reverse the effects of many T2D related metabolic changes, to our surprise in the working T2D like model, over-expression of Grb2, instead of reducing the activity of ROS, rather elevated it by 3.57 fold (Figure 7E,F). Nevertheless, the extent of this limited fate reversal upon Grb2 overexpression was estimated, and in both Palmitate and Amylin treated situations, Grb2 overexpression up-regulated the expressions of cytoskeletal proteins significantly.
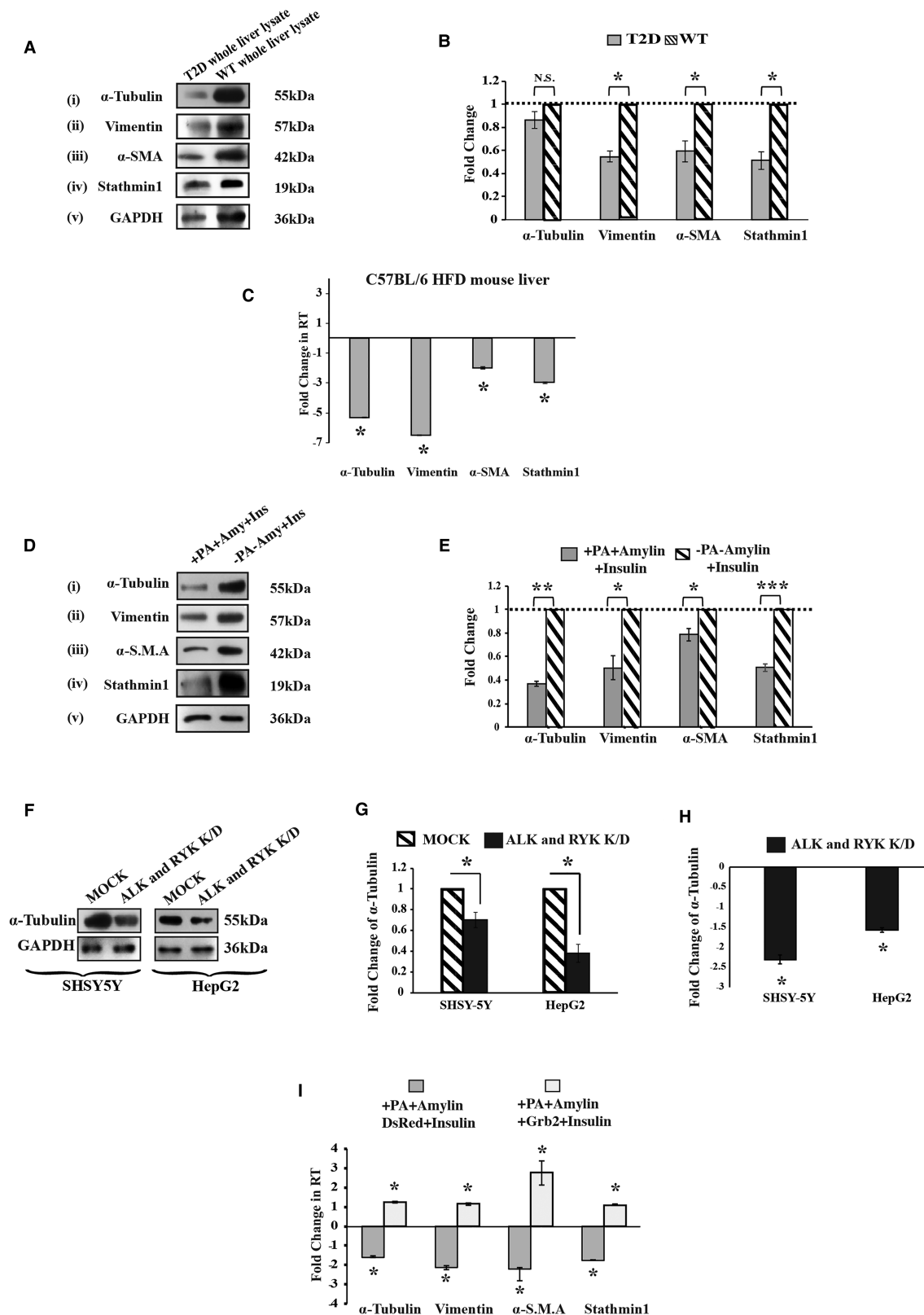
Figure 5. Participation of ALK and RYK in signaling events leading to cytoskeleton degradation and Grb2 mediated reversal in T2D: cytoskeleton degradation.

Part 1 of 2

(**A**) Representative western blots (n = 2) of four cytoskeletal proteins (**i**) α-Tubulin, (**ii**) Vimentin, (**iii**) α-SMA and (**iv**) Stathmin1 with (**v**) GAPDH used as

Figure 5. Participation of ALK and RYK in signaling events leading to cytoskeleton degradation and Grb2 mediated reversal in T2D: cytoskeleton degradation.

internal control in human diabetic whole liver lysates, compared with wild type whole liver lysate. (**B**) Histogram representing the mean value of optical density of the protein bands, normalized against GAPDH, with a decrease in 1.16 fold for α-Tubulin, 1.83 fold for Vimentin, 1.68 fold for α-SMA and 1.95 fold for Stathmin1. Samples are derived from the same experiments and the blots are processed in parallel. (**C**) Shows transcript level changes in α-Tubulin (−5.3 fold), Vimentin (−6.49 fold), α-SMA (−2 fold), and Stathmin1 (−2.9 fold) by qRT-PCR in C57BL/6 mice on OWD compared with normal diet fed controls. (**D**) Western blots depict alteration in the expression of (**i**) α-Tubulin, (**ii**) Vimentin, (**iii**) α-Smooth muscle actin (α-SMA) and (**iv**) Stathmin1with GAPDH in T2D cell model (PA, +Amylin, +Insulin induced HepG2 cells). The samples are derived from the same experiments and the blots are processed in parallel. (**E**) Histograms showing changes in the four cytoskeletal proteins, normalized by GAPDH, with decrease 2.7 fold for α-Tubulin, 1.98 for Vimentin, 1.27 fold for α-SMA and 1.97 fold for Stathmin1. ALK and RYK double knockdown condition controls α-Tubulin degradation. (**F** and **G**) shows in western blot, the decrease in α-Tubulin in both SHSY-5Y [−2.64 fold] and HepG2 cell line [−1.42 fold] in ALK and RYK double knockdown (K/D) situation. (**H**) shows the α-Tubulin transcript level down-regulation in ALK and RYK double knockdown (K/D) model in both SHSY5Y [−2.3 fold] and HepG2 cell lines [−1.5 fold] by qRT-PCR. (**I**) Shows transcript level changes for the four cytoskeletal proteins in T2D (PA +Amyli +Insulin induced condition) with or without Grb2.All the statistical information is available on Supplementary Table S7.

Discussion

This work unveils the commonality of two diverse diseases, AD and T2D. Despite efforts to relate the two for more than a decade, none of the studies focused on the signaling components and their possible convergence on a transcription factor.

The precise common signaling mechanism for AD and T2D is still unclear, albeit the fact that both the diseases confer insulin resistance. Up until our recent work, Insulin Receptor (IR) family was the only RTKs known to be involved in the signaling in both the diseases [6]. Profiling the activities of other RTKs in the two diseases opened up a larger picture and the effects of both Aβ and Amylin oligomers were predicted to have impacts on other receptor tyrosine kinases [6].

Amongst all the common RTKs, ALK and RYK were the two showing similar levels of deactivation in all working models of AD and T2D [6]. ALK, a member of insulin receptor superfamily, is commonly known for its involvement in many cancer types, especially in non-small-cell lung cancer (NSCLC) [63]. RYK is a co-receptor of non-canonical Wnt signaling [64]. The involvement of Wnt signaling pathway in AD [65] and T2D [66,67] is well established. We further verified the association of classical Wnt pathway through the down-regulation of β-Catenin (Figure 4C–F) and up-regulation of GSK3β [6,19] in both diseases. This is a significant revelation considering that α-Tubulin is down-regulated in T2D conditions, and that the activity of Gsk3β, a kinase that would hyperphosphorylate Tau leading to destabilization of the microtubule network, increases under disease inducing Palmitate/Amylin treatment [6]. The activity of its upstream effector AKT1 also decreases under T2D inducing condition [6].

Recent reports and our real-time PCR data (Figure 1I,J) have revealed the active involvement of miR-1271 in both the diseases, AD [34] and T2D [35]. miR-1271 and miR-96 are known paralogs to each other [68]. The mirDB [61] target analysis of of both miR-1271 (Supplementary Information S1) and miR-96 (Supplementary Information S2) have also confirmed their roles in the ALK and RYK down-regulation. This observation is further corroborated by Kong et al., who have demonstrated ALK as the target for miR-1271 in oral squamous cell carcinoma (OSCC) [69]. RYK was observed as a target gene for miR-96, the paralog of miR-1271 [68,70,71]. Additionally, the expression of miR-96 is also up-regulated in Alzheimer's disease [72]. Up-regulated expression of miR-1271, or its paralog, in both the diseases, and their targeting of both ALK and RYK are well perceived. The mirDB [61] analysis further demonstrated that mechanistic target of rapamycin (mTOR) is targeted by both miR-1271 and miR-96 [Supplementary Information 1 and 2]. Several studies confirmed that down-regulation of mTOR led to autophagy [73–75]. Concomitantly, both AD [76] and T2D [77] induced autophagy by the inhibition of mTOR protein. Thus, the elevated levels of miR-1271 could affect both AD and T2D not only by ALK/RYK, but also through the mTOR/autophagy pathway. Furthermore, the gene-hancer analysis revealed SP1 (specificity protein 1) as one of the putative transcription factors of miR-1271. Besides, the role of SP1 in the expression of several AD-related proteins, including amyloid-β protein precursor
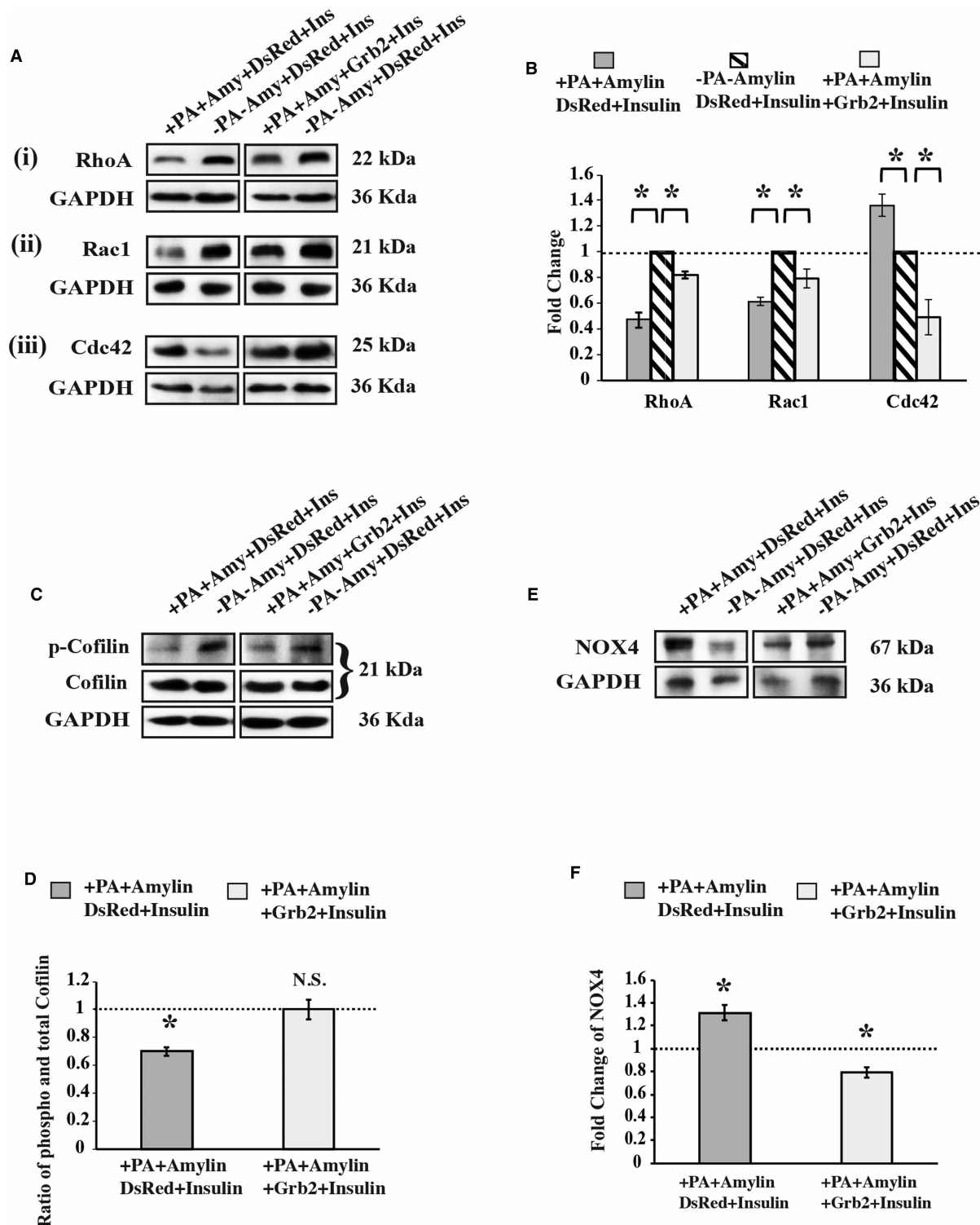
Figure 6. Signaling molecules participate in T2D.

(**A**) Western blot showing protein level changes of small GTPases i.e. (**i**) RhoA [−2.13 fold and in presence of Grb2 −1.22 fold], (**ii**) Rac1 [−1.63 fold and in presence of Grb2 −1.26 fold] and (**iii**) CDC42 [+1.36 fold and in presence of Grb2 −2.05 fold] in T2D inducing (+PA, +Amylin, +Insulin in HepG2 cells) and in reversing conditions (+PA, +Amylin, +Insulin, +Grb2 in HepG2 cells). In (**B**) Bar diagram represents the activity alterations for the small GTPases. (**C** and **D**) Western blots depict the protein levels or activation of signaling molecules like Cofilin [−1.43 fold]. (**E** and **F**) depictNOX4 [+1.31 fold and in presence of Grb2 −1.26 fold] by Western blot. All the statistical information is available in Supplementary Table S7.

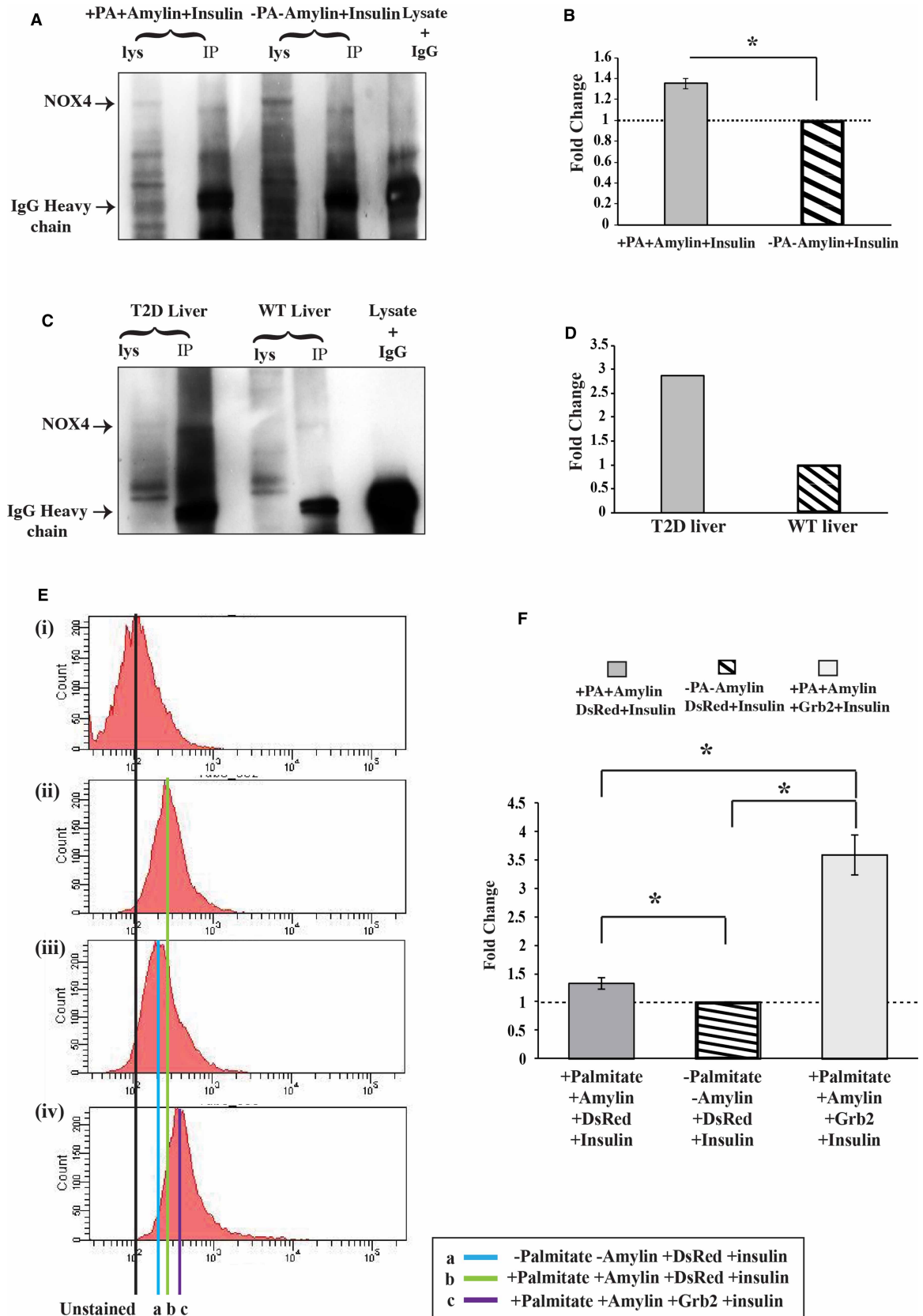**Figure 7. Grb2 and NOX4 interaction prevents cytoskeletal degradation in T2D like scenario and ROS activity.** Part 1 of 2
(**A**) shows the variation of interaction of Grb2 and NOX4 in T2D inducing (+Palmitate, +Amylin and +Insulin in HepG2) conditions

PORTLAND
PRESS

Figure 7. Grb2 and NOX4 interaction prevents cytoskeletal degradation in T2D like scenario and ROS activity. Part 2 of 2
compared with controls (−Palmitate, −Amylin and +Insulin in HepG2). (**B**) graphical representation of the intensity of the
interaction between NOX4 and Grb2. (**C**) shows the variation of interaction of Grb2 and NOX4 in type 2 diabetic mouse (OWD
C57BL/6) whole liver lysate compared with WT (Normal fed C57BL/6) control. (**D**) graphical representation of the intensity of the
interaction between NOX4 and Grb2 in T2D mouse liver lysate. ROS activity Assay. (**E**) (**i**), (**ii**), (**iii**) and (**iv**) show the FACS data
for ROS activity of unstained, −Palmitate −Amylin +DsRed +Insulin, +Palmitate, +Amylin, +DsRed, +Insulin and +Palmitate,
+Amylin, +Grb2, +Insulin, respectively, in HepG2 cells. (**F**) Shows graphically that ROS activity increases in T2D inducing
(+Palmitate, +Amylin, +DsRed, +Insulin) condition by 1.3 fold and in presence of Grb2 ROS activity further significantly
increases by 3.5 fold. All the statistical information is available on Supplementary Table S7.

(APP), BACE1 and tau is well documented [78,79]. Similarly, SP1 plays a crucial role in the development of
insulin resistance in T2D [80,81]. Therefore, elevated levels of SP1 could be the reason behind up-regulation of
miR-1271.

Grb2 happens to be a common downstream adapter for both the RTKs [63,82]. It was shown previously that
Grb2 strengthened its interaction with NOX4 to rescue the cytoskeleton degradation in AD like situations [19].
We postulate that the two RTKs, ALK and RYK, might act like non-canonical receptors with the potential to
become a significant link between AD and T2D via Grb2 and NOX4.

The downstream consequences at the molecular level for both the signals were significant compromise of
cytoskeleton integrity. Interestingly, ALK and RYK double knockdown cell lines also resembled similar phe-
notypes (Figure 5F–H). Searching for molecules that could connect the common RTKs with downstream
cytoskeleton degradation, we singled out Grb2 and NOX4, both of which had elevated levels in the disease

Table 1 A summary of status of dysregulated proteins in AD and T2D disease conditions

| SI No.	Name of protein	Upstream effector/effect	Downstream effector/effect	Status in disease condition AD	T2D
1	ALK	miR-1271	Grb2, NOX4	↓[6]	↓[6]
2	RYK	miR-1271	Grb2, NOX4	↓[6]	↓[6]
3	Grb2	ALK, RYK, PAX4	Recover Cytoskeleton Proteins degradation after Grb2–NoX4 interaction	↑[19]	↑
4	NOX4	Reactive Oxygen Species (ROS) [95], Rac1 [96], ALK, RYK, PAX4	SSH-1 [18,19], Recover Cytoskeleton Proteins degradation after Grb2–NoX4 interaction	↑[19]	↑
5	PAX4	ARX	Grb2, NOX4	↑	↑
6	ARX	β-Catenin	PAX4	↓	↓
7	β-Catenin	GSK3β	ARX	↓	↓
8	GSK3β activity	AKT1	β-Catenin	↑[6]	↑[6]
9	AKT1 activity	PTEN [97]	GSK3β	↓[6]	↓[6]
10	Cytoskeleton Proteins (α-Tubulin, Vimentin, α-SMA, Stathmin1)	RhoA, Rac1 and C dc 42	Degeneration of cell	↓[19]	↓
11	RhoA	AKT1 [98]	Cytoskeleton proteins	↓[19]	↓
12	Rac1	AKT1 [98]	Cytoskeleton proteins	↓[19]	↓
13	Cdc42	AKT1 [98]	Cytoskeleton proteins	↑[19]	↑
14	Cofilin activity	LIMK [99]	F-Actin	↓[19]	↓
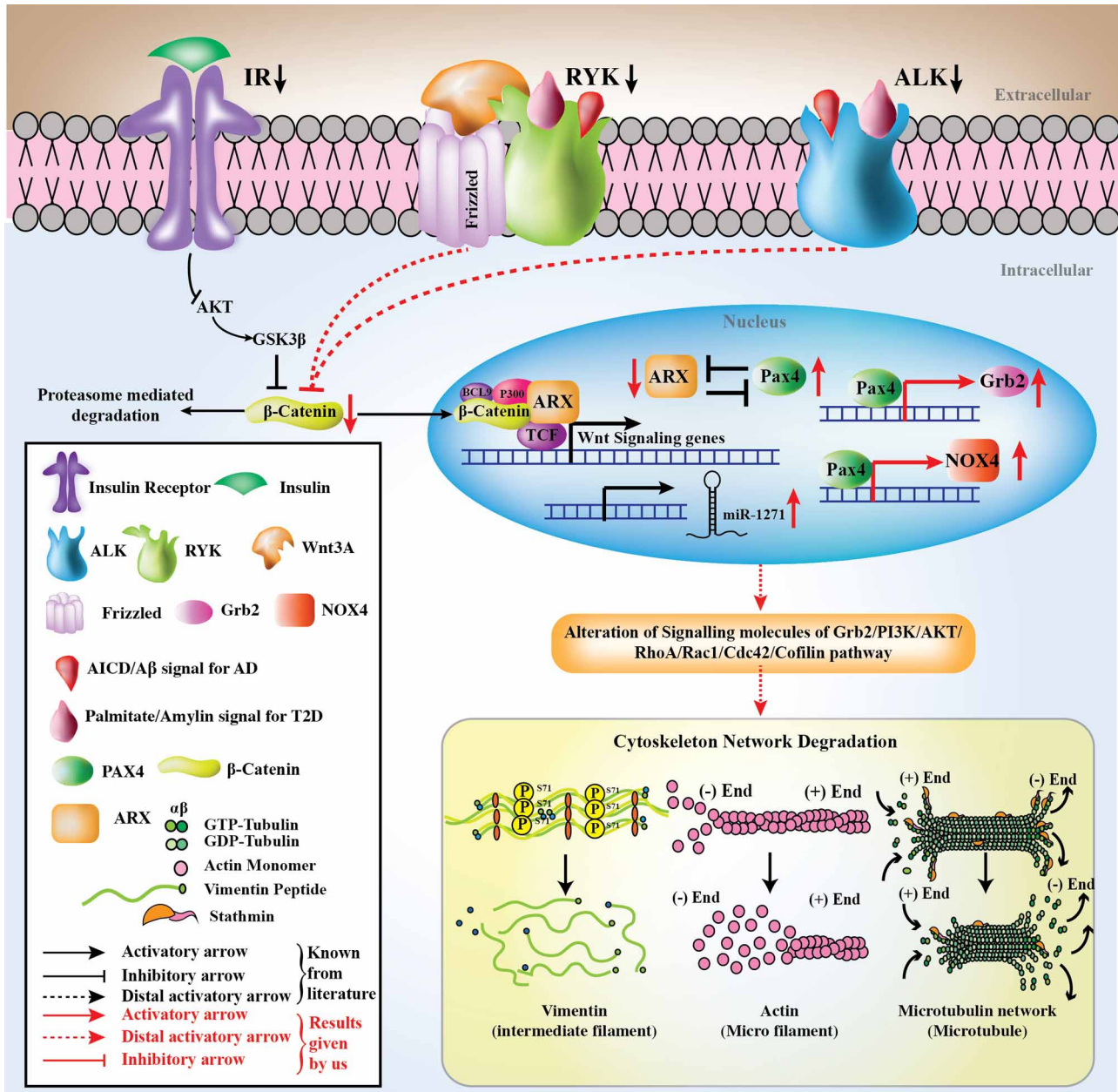
Figure 8. Summary diagram.

A cartoon representation summarizing the overlap of signaling pathways for both AD and T2D, mediated via the down-regulation of membrane bound ALK/RYK, consequent up-regulation of the transcription factor PAX4, which in turn up-regulates Grb2/NOX4. These effectors, through the signaling molecules, affect the fate of the cytoskeletal proteins.

scenarios (Figure 1; Supplementary Figures S2–S4). Several reports on Grb2 strongly suggested its role in cellular survival in AD [55,57]. Transcript levels of the cytoskeletal protein components were checked and were found to increase several folds with Grb2's overexpression in both AD [19] and T2D models (Figure 5I).

It was prudent therefore to try to understand the underpinning cellular mechanisms that help in the cyto-skeletal restructuring, with possibly Grb2 playing a pivotal role. The expressions of three small GTPases, RhoA, Rac1 and Cdc42, known to regulate cell morphology through rearrangement of cytoskeletal proteins [83–85]

acting as molecular switches, were significantly altered and again renormalized with overexpression of Grb2. These alterations in the activities of small GTPases were sufficient to perturb the downstream signaling events and, ultimately, the cytoskeletal proteins were degraded primarily through Cofilin mediated mechanism. Cofilin is a downstream effector of RhoA, Rac1 and Cdc42 and it is one of the actin-binding proteins whose dephosphorylation enables actin depolymerization [86]. These results convincingly implies similar pathways for the rearrangement of the cytoskeleton network in AD and T2D. Grb2's intervention in both disease models significantly inactivates Cofilin by phosphorylation [19] (Figure 6C,D), a crucial regulator of actin dynamics [87]. Similar to the case in AD, in T2D also Grb2 helps reversing the signals involved in the degradation of cytoskeletal proteins.

Abnormal NOX activation is already reported in T2D [88] leading to its interaction with Grb2 and Src activation [18]. Adapter protein NOX4, from the ROS production pathway, is another Cofilin regulator in conjunction with Slingshot homolog-1 (SSH-1), the phosphatase of Cofilin. Both the disease models showed significant up-regulation of NOX4 (Figure 6E,F), which was subsequently decreased with Grb2's overexpression [19]. These small checks and balances, at different levels along the signaling cascades, culminated in a larger scale perturbation in the cytoskeleton network and Grb2's role emerged as a reversing switch of these perturbations (Figure 5I) [19]. Furthermore, while examining other effects on cytoskeleton integrity due to Grb2's overexpression, it was noted that NOX4 interacted with Grb2 in normal conditions [17,18] which increased several folds under both AD [19] and T2D disease conditions (Figure 7A–D). As NOX4 was responsible for ROS generation, we also checked whether Grb2 overexpression could put a check on the ROS, which it could not. On the contrary, the ROS activity had increased in the presence of too much of Grb2 (Figure 7E,F). This might be a hint towards the fact that even though the cells geared up the protective mechanisms, the defense was lost with the progression of the disease and beyond a threshold.

The study unraveled the relation of ALK and RYK in controlling the cytoskeleton integrity through the overexpression of Grb2 and NOX4 (Supplementary Figure S6), with miR-1271 as the master-regulator controlling ALK/RYK expression (Supplementary Information S1; Figure 1I,J). Employing bioinformatics tools and qRT-PCR, we identified PAX4 as a central regulator (Supplementary Tables S5,S6; Figures 2A,B,F–H, 3A, B), which is also crucial in regulating the gene network governing β-cell mass expansion and survival under the pathophysiological conditions of T2D [89]. Recent studies have shown association of *PAX4* mutations with T2D in Japanese and Afro-Americans populations [42,90]. However, *PAX4* gene dysfunction increases the susceptibility of apoptosis along with reducing cell proliferation leading to a gradual loss of β-cell and ultimately to diabetes [89]. Interestingly, the PI3K inhibitor, Wortmannin, showed potential to induce both insulin resistance and PAX4 expression [89,91]. Naturally, *PAX4* emerged as a survival gene because of its role in regulating both β-cell mass expansion and Grb2 expression. On the other hand, the antagonism between PAX4 and ARX (Figure 4A) could connect the aberrant Wnt/β-Catenin signaling with the up-regulation of PAX4 via reduction in ARX in both the diseases (Figure 4B). This helps connect the dots between the deactivation of ALK and RYK with the down-regulation of β-Catenin expression (Figure 4C–F) levels, followed by a decrease in ARX. Thus, down-regulation of ALK and RYK implies an elevation of the PAX4 level (Figures 2C–E, 3C–E; Supplementary Figure S8), which in turn up-regulates Grb2 and NOX4 in both AD and T2D.

NOX4 reportedly induces mitochondrial dysfunction by inhibiting the mitochondrial chain complex 1 [92]. Alterations in the expression of genes coding for mitochondrial and cytoskeletal proteins contribute to the mitochondrial dysfunction observed in insulin-resistant conditions of both AD and T2D [93,94]. Interestingly, the majority of differentially expressed genes targeted by *PAX4* are commonly enriched in both oxidative phosphorylation and neurodegenerative diseases [45]. Besides, this work establishes PAX4 as a promising candidate behind up-regulation of *GRB2* and *NOX4* in T2D, acting as the coveted 'missing link' between AD and T2D's common signaling pathways (Figures 2C–H, 3C–G; Supplementary Figure S8). Like a pivot, it links ALK, RYK as upstream receptors and Grb2, NOX4 as downstream adapters, eventually affecting the cytoskeleton. The status of all the dysregulated proteins involved in this study are compiled in Table 1.

In the context of Insulin Receptor (IR) insensitivity being the pathological hallmark of both diseases, previous findings called for understanding the roles of other members of the RTK family. For the first time two non-canonical receptors (ALK or RYK) have been shown to link disparate signals (AICD/Aβ and Palmitate/Amylin) leading to similar pathways (Grb2/PI3K/AKT/RhoA/Rac1/Cdc42/Cofilin or NOX4/SSH-1/Cofilin) that ultimately culminate in similar mechanistic consequences (degradation of cytoskeleton network) (Figure 8; Supplementary Figure S9).

Conclusions

The emerging model from this study would help understand both the diseases from each other's perspectives. The work unraveled (a) a novel avenue to study the implications of other RTKs, besides IR, for both the diseases, (b) the unique role of Grb2 and NOX4 in the management of cytoskeleton degradation under AD/T2D conditions and (c) most importantly, the emergence of PAX4 as the first Transcription Factor that actively regulates the pathways of both AD and T2D.

Data Availability

There are no large data sets associated with this manuscript. Reagents described in this study available on reasonable request.

Competing Interests

The authors declare that there are no competing interests associated with the manuscript.

Funding

CRediT Author Contribution

Debashis Mukhopadhyay: Conceptualization, Resources, Formal analysis, Supervision, Funding acquisition, Validation, Investigation, Visualization, Project administration, Writing — review and editing. **Piyali Majumder:** Conceptualization, Data curation, Software, Formal analysis, Investigation, Methodology, Writing — original draft, Writing — review and editing. **Kaushik Chanda:** Data curation, Methodology. **Debajyoti Das:** Data curation, Methodology. **Brijesh Kumar Singh:** Methodology. **Partha Chakrabarti:** Resources, Data curation, Methodology. **Nihar Ranjan Jana:** Resources, Methodology.

Abbreviations

AD, Alzheimer's Disease; ALK, anaplastic lymphoma kinase; APP, amyloid precursor protein; ARX, Aristaless Related Homeobox; IR, insulin receptor; PAX4, Paired Box Protein 4; ROS, reactive oxygen species; RTK, receptor tyrosine kinase; RYK, Receptor-like Tyrosine Kinase; SMA, smooth muscle actin; SSH-1, Slingshot homolog-1; TF, transcription factors.

References

1 Barbagallo, M. and Dominguez, L.J. (2014) Type 2 diabetes mellitus and Alzheimer's disease. *World J. Diabetes* **5**, 889–893 https://doi.org/10.4239/wjd.v5.i6.889

2 Umegaki, H. (2014) Type 2 diabetes as a risk factor for cognitive impairment: current insights. *Clin. Interv. Aging* **9**, 1011–1019 https://doi.org/10.2147/CIA.S48926

3 Marzban, L., Park, K. and Verchere, C.B. (2003) Islet amyloid polypeptide and type 2 diabetes. *Exp. Gerontol.* **38**, 347–351 https://doi.org/10.1016/S0531-5565(03)00004-4

4 Wilson, C.M., Magnaudeix, A., Yardin, C. and Terro, F. (2014) Autophagy dysfunction and its link to Alzheimer's disease and type II diabetes mellitus. *CNS Neurol. Disord. Drug Targets* **13**, 226–246 https://doi.org/10.2174/18715273113126660146

5 Mittal, K., Mani, R.J. and Katare, D.P. (2016) Type 3 diabetes: cross talk between differentially regulated proteins of type 2 diabetes mellitus and Alzheimer's disease. *Sci. Rep.* **6**, 25589 https://doi.org/10.1038/srep25589

6 Majumder, P., Roy, K., Bagh, S. and Mukhopadhyay, D. (2019) Receptor tyrosine kinases (RTKs) consociate in regulatory clusters in Alzheimer's disease and type 2 diabetes. *Mol. Cell. Biochem.* **459**, 171–182 https://doi.org/10.1007/s11010-019-03560-5

7 Anand, M., Lai, R. and Gelebart, P. (2011) β-catenin is constitutively active and increases STAT3 expression/activation in anaplastic lymphoma kinase-positive anaplastic large cell lymphoma. *Haematologica* **96**, 253–261 https://doi.org/10.3324/haematol.2010.027086

8 Adamo, A., Fiore, D., De Martino, F., Roscigno, G., Affinito, A., Donnarumma, E., et al. (2017) RYK promotes the stemness of glioblastoma cells via the WNT/β-catenin pathway. *Oncotarget* **8**, 13476–13487 https://doi.org/10.18632/oncotarget.14564

9 Roy, J.P., Halford, M.M. and Stacker, S.A. (2018) The biochemistry, signalling and disease relevance of RYK and other WNT-binding receptor tyrosine kinases. *Growth Factors* **36**, 15–40 https://doi.org/10.1080/08977194.2018.1472089

10 Norwitz, N.G., Mota, A.S., Norwitz, S.G. and Clarke, K. (2019) Multi-loop model of Alzheimer disease: an integrated perspective on the Wnt/GSK3β, α-synuclein, and type 3 diabetes hypotheses. *Front. Aging Neurosci.* **11**, 184 https://doi.org/10.3389/fnagi.2019.00184

11 Llorens-Martín, M., Jurado, J., Hernández, F. and Avila, J. (2014) GSK-3β, a pivotal kinase in Alzheimer disease. *Front. Mol. Neurosci.* **7**, 46 https://doi.org/10.3389/fnmol.2014.00046

12 Inestrosa, N.C. and Toledo, E.M. (2008) The role of Wnt signaling in neuronal dysfunction in Alzheimer's disease. *Mol. Neurodegener.* **3**, 9 https://doi.org/10.1186/1750-1326-3-9

13 Ciaraldi, T.P., Oh, D.K., Christiansen, L., Nikoulina, S.E., Kong, A.P.S., Baxi, S. et al. (2006) Tissue-specific expression and regulation of GSK-3 in human skeletal muscle and adipose tissue. *Am. J. Physiol. Endocrinol. Metab.* **291**, E891–E898 https://doi.org/10.1152/ajpendo.00176.2006

14   Macheda, M.L., Sun, W.W., Kugathasan, K., Hogan, B.M., Bower, N.I., Halford, M.M., et al. (2012) The Wnt receptor Ryk plays a role in mammalian planar cell polarity signaling. *J. Biol. Chem.* **287**, 29312–29323 https://doi.org/10.1074/jbc.M112.362681

15   Gobbo, M.G., Ribeiro, D.L., Taboga, S.R., Almeida, D., Alves, E. and Góes, R.M. (2012) Oxidative stress markers and apoptosis in the prostate of diabetic rats and the influence of vitamin C treatment. *J. Cell. Biochem.* **113**, 2223–2233 https://doi.org/10.1002/jcb.24092

16   Diaz, B., Shani, G., Pass, I., Anderson, D., Quintavalle, M. and Courtneidge, S.A. (2009) Tks5-dependent, Nox-mediated generation of reactive oxygen species is necessary for invadopodia formation. *Sci. Signal.* **2**, ra53 https://doi.org/10.1126/scisignal.2000368

17   Montenegro, M.F., Valdivia, A., Smolensky, A., Verma, K., Taylor, W.R. and San Martín, A. (2015) Nox4-dependent activation of cofilin mediates VSMC reorientation in response to cyclic stretching. *Free Radic. Biol. Med.* **85**, 288–294 https://doi.org/10.1016/j.freeradbiomed.2015.05.011

18   Xi, G., Shen, X.-C., Wai, C. and Clemmons, D.R. (2013) Recruitment of Nox4 to a plasma membrane scaffold is required for localized reactive oxygen species generation and sustained Src activation in response to insulin-like growth factor-I. *J. Biol. Chem.* **288**, 15641–15653 https://doi.org/10.1074/jbc.M113.456046

19   Majumder, P., Roy, K., Singh, B.K., Jana, N.R. and Mukhopadhyay, D. (2017) Cellular levels of Grb2 and cytoskeleton stability are correlated in a neurodegenerative scenario. *Dis. Model. Mech.* **10**, 655–669 https://doi.org/10.1242/dmm.027748

20   Bruce-Keller, A.J., Gupta, S., Knight, A.G., Beckett, T.L., McMullen, J.M., Davis, P.R. et al. (2011) Cognitive impairment in humanized APP×PS1 mice is linked to Aβ(1-42) and NOX activation. *Neurobiol. Dis.* **44**, 317–326 https://doi.org/10.1016/j.nbd.2011.07.012

21   Shimohama, S., Tanino, H., Kawakami, N., Okamura, N., Kodama, H., Yamaguchi, T., et al. (2000) Activation of NADPH oxidase in Alzheimer's disease brains. *Biochem. Biophys. Res. Commun.* **273**, 5–9 https://doi.org/10.1006/bbrc.2000.2897

22   Wu, X. and Williams, K.J. (2012) The NOX4 pathway as a source of selective insulin resistance and responsiveness. *Arterioscler. Thromb. Vasc. Biol.* **32**, 1236–1245 https://doi.org/10.1161/ATVBAHA.111.244525

23   Gorin, Y. and Block, K. (2013) Nox4 and diabetic nephropathy: with a friend like this who needs enemies. *Free Radic. Biol. Med.* **61**, 130–142 https://doi.org/10.1016/j.freeradbiomed.2013.03.014

24   Opie, E.L. (1901) On the relation of chronic interstitial pancreatitis to the islands of langerhans and to diabetes melutus. *J. Exp. Med.* **5**, 397–428 https://doi.org/10.1084/jem.5.4.397

25   Bower, R.L. and Hay, D.L. (2016) Amylin structure–function relationships and receptor pharmacology: implications for amylin mimetic drug development. *Br. J. Pharmacol.* **173**, 1883–1898 https://doi.org/10.1111/bph.13496

26   Renner, M., Lacor, P.N., Velasco, P.T., Xu, J., Contractor, A., Klein, W.L. et al. (2010) Deleterious effects of amyloid β oligomers acting as an extracellular scaffold for mGluR5. *Neuron* **66**, 739–754 https://doi.org/10.1016/j.neuron.2010.04.029

27   Ge, X., Yang, Y., Sun, Y., Cao, W. and Ding, F. ((2018) Islet amyloid polypeptide promotes amyloid-beta aggregation by binding-induced helix-unfolding of the amyloidogenic core. *ACS Chem. Neurosci.* **9**, 967–975 https://doi.org/10.1021/acschemneuro.7b00396

28   Moreno-Gonzalez, I., Edwards Iii, G., Salvadores, N., Shahnawaz, M., Diaz-Espinoza, R. and Soto, C. (2017) Molecular interaction between type 2 diabetes and Alzheimer's disease through cross-seeding of protein misfolding. *Mol. Psychiatry.* **22**, 1327–1334 https://doi.org/10.1038/mp.2016.230

29   Bakou, M., Hille, K., Kracklauer, M., Spanopoulou, A., Frost, C.V., Malideli, E. et al. (2017) Key aromatic/hydrophobic amino acids controlling a cross-amyloid peptide interaction versus amyloid self-assembly. *J. Biol. Chem.* **292**, 14587–14602 https://doi.org/10.1074/jbc.M117.774893

30   Hu, R., Zhang, M., Chen, H., Jiang, B. and Zheng, J. (2015) Cross-seeding interaction between β-amyloid and human islet amyloid polypeptide. *ACS Chem. Neurosci.* **6**, 1759–1768 https://doi.org/10.1021/acschemneuro.5b00192

31   Yan, L.M., Velkova, A. and Kapurniotu, A. (2014) Molecular characterization of the hetero-assembly of β-amyloid peptide with islet amyloid polypeptide. *Curr. Pharm. Des.* **20**, 1182–1191 https://doi.org/10.2174/13816128113199990064

32   Andreetto, E., Yan, L.M., Tatarek-Nossol, M., Velkova, A., Frank, R. and Kapurniotu, A. (2010) Identification of hot regions of the abeta-IAPP interaction interface as high-affinity binding sites in both cross- and self-association. *Angew. Chem. Int. Ed. Engl.* **49**, 3081–3085 https://doi.org/10.1002/anie.200904902

33   Rezaei-Ghaleh, N., Andreetto, E., Yan, L.M., Kapurniotu, A. and Zweckstetter, M. (2011) Interaction between amyloid beta peptide and an aggregation blocker peptide mimicking islet amyloid polypeptide. *PLoS ONE* **6**, e20289 https://doi.org/10.1371/journal.pone.0020289

34   Chanda, K., Laha, S., Chatterjee, R. and Mukhopadhyay, D. (2021) Amyloid precursor protein intra-cellular domain (AICD), Aß and their confounding synergistic effects differentially regulate the degradome of cellular models of Alzheimer's disease. *Gene Rep.* **23**, https://doi.org/10.1016/j.genrep.2021.101082

35   Yang, W.-M., Min, K.-H. and Lee, W. (2016) MiR-1271 upregulated by saturated fatty acid palmitate provokes impaired insulin signaling by repressing INSR and IRS-1 expression in HepG2 cells. *Biochem. Biophys. Res. Commun.* **478**, 1786–1791 https://doi.org/10.1016/j.bbrc.2016.09.029

36   Lorenzo, P.I., Cobo-Vuilleumier, N. and Gauthier, B.R. (2018) Therapeutic potential of pancreatic PAX4-regulated pathways in treating diabetes mellitus. *Curr. Opin. Pharmacol.* **43**, 1–10 https://doi.org/10.1016/j.coph.2018.07.004

37   Brun, T., Hu He, K.H., Lupi, R., Boehm, B., Wojtusciszyn, A., Sauter, N. et al. (2008) The diabetes-linked transcription factor Pax4 is expressed in human pancreatic islets and is activated by mitogens and GLP-1. *Hum. Mol. Genet.* **17**, 478–489 https://doi.org/10.1093/hmg/ddm325

38   Napolitano, T., Avolio, F., Courtney, M., Vieira, A., Druelle, N., Ben-Othman, N. et al. (2015) Pax4 acts as a key player in pancreas development and plasticity. *Semin. Cell Dev. Biol.* **44**, 107–114 https://doi.org/10.1016/j.semcdb.2015.08.013

39   Collombat, P., Mansouri, A., Hecksher-Sørensen, J., Serup, P., Krull, J., Gradwohl, G. et al. (2003) Opposing actions of Arx and Pax4 in endocrine pancreas development. *Genes Dev.* **17**, 2591–2603 https://doi.org/10.1101/gad.269003

40   Djiotsa, J., Verbruggen, V., Giacomotto, J., Ishibashi, M., Manning, E., Rinkwitz, S. et al. (2012) Pax4 is not essential for beta-cell differentiation in zebrafish embryos but modulates alpha-cell generation by repressing arx gene expression. *BMC Dev. Biol.* **12**, 37 https://doi.org/10.1186/1471-213X-12-37

41   Gage, B.K., Baker, R.K. and Kieffer, T.J. (2014) Overexpression of PAX4 reduces glucagon expression in differentiating hESCs. *Islets* **6**, e29236 https://doi.org/10.4161/isl.29236

42   Shimajiri, Y., Sanke, T., Furuta, H., Hanabusa, T., Nakagawa, T., Fujitani, Y. et al. (2001) A missense mutation of Pax4 gene (R121W) is associated with type 2 diabetes in Japanese. *Diabetes* **50**, 2864–2869 https://doi.org/10.2337/diabetes.50.12.2864

43   Lorenzo, P.I., Juárez-Vicente, F., Cobo-Vuilleumier, N., García-Domínguez, M. and Gauthier, B.R. (2017) The diabetes-linked transcription factor PAX4: from gene to functional consequences. *Genes* **8**, 101 https://doi.org/10.3390/genes8030101

44 Volodin, A., Kosti, I., Goldberg, A.L. and Cohen, S. (2017) Myofibril breakdown during atrophy is a delayed response requiring the transcription factor PAX4 and desmin depolymerization. *Proc. Natl Acad. Sci. U.S.A.* **114**, E1375–E1384 https://doi.org/10.1073/pnas.1612988114

45 Kong, P., Lei, P., Zhang, S., Li, D., Zhao, J. and Zhang, B. (2018) Integrated microarray analysis provided a new insight of the pathogenesis of Parkinson's disease. *Neurosci. Lett.* **662**, 51–58 https://doi.org/10.1016/j.neulet.2017.09.051

46 Cho, I.-T., Lim, Y., Golden, J.A. and Cho, G. (2017) Aristaless related homeobox (ARX) interacts with β-catenin, BCL9, and P300 to regulate canonical Wnt signaling. *PLoS ONE* **12**, e0170282 https://doi.org/10.1371/journal.pone.0170282

47 Ghadami, S. and Eshaghkhani, Y. (2019) ARX gene with an impressive role in X-linked intellectual disability. *J. Genet. Mol. Biol.* **3**, 1–10 https://doi.org/10.1016/j.genrep.2021.101082

48 Absoud, M., Parr, J.R., Halliday, D., Pretorius, P., Zaiwalla, Z. and Jayawant, S. (2010) A novel ARX phenotype: rapid neurodegeneration with ohtahara syndrome and a dyskinetic movement disorder. *Dev. Med. Child Neurol.* **52**, 305–307 https://doi.org/10.1111/j.1469-8749.2009.03470.x

49 Nagy, Z., Esiri, M.M. and Smith, A.D. (1998) The cell division cycle and the pathophysiology of Alzheimer's disease. *Neuroscience* **87**, 731–739 https://doi.org/10.1016/S0306-4522(98)00293-0

50 Wang, W., Bu, B., Xie, M., Zhang, M., Yu, Z. and Tao, D. (2009) Neural cell cycle dysregulation and central nervous system diseases. *Prog. Neurobiol.* **89**, 1–17 https://doi.org/10.1016/j.pneurobio.2009.01.007

51 McShea, A., Zelasko, D.A., Gerst, J.L. and Smith, M.A. (1999) Signal transduction abnormalities in Alzheimer's disease: evidence of a pathogenic stimuli. *Brain Res.* **815**, 237–242 https://doi.org/10.1016/S0006-8993(98)01135-4

52 Ghate, P.S., Sidhar, H., Carlson, G.A. and Giri, R.K. (2014) Development of a novel cellular model of Alzheimer's disease utilizing neurosphere cultures derived from B6C3-Tg(APPswe,PSEN1dE9)85Dbo/J embryonic mouse brain. *SpringerPlus* **3**, 161 https://doi.org/10.1186/2193-1801-3-161

53 Baksi, S., Jana, N.R., Bhattacharyya, N.P. and Mukhopadhyay, D. (2013) Grb2 is regulated by Foxd3 and has roles in preventing accumulation and aggregation of mutant huntingtin. *PLOS ONE* **8**, e76792 https://doi.org/10.1371/journal.pone.0076792

54 Raychaudhuri, M. and Mukhopadhyay, D. (2007) AICD and its adaptors: in search of new players. *J. Alzheimers Dis.* **11**, 343–358 https://doi.org/10.3233/JAD-2007-11311

55 Raychaudhuri, M. and Mukhopadhyay, D. (2010) Grb2-mediated alteration in the trafficking of AbetaPP: insights from Grb2-AICD interaction. *J. Alzheimers Dis.* **20**, 275–292 https://doi.org/10.3233/JAD-2010-1371

56 Raychaudhuri, M., Roy, K., Das, S. and Mukhopadhyay, D. (2012) The N-terminal SH3 domain of Grb2 is required for endosomal localization of AβPP. *J. Alzheimers Dis.* **32**, 479–493 https://doi.org/10.3233/JAD-2012-120388

57 Roy, K., Raychaudhuri, M., Chakrabarti, O. and Mukhopadhyay, D. (2014) Growth factor receptor-bound protein 2 promotes autophagic removal of amyloid-β protein precursor intracellular domain overload in neuronal cells. *J. Alzheimers Dis.* **38**, 881–895 https://doi.org/10.3233/JAD-130929

58 Dahlgren, K.N., Manelli, A.M., Stine, W.B., Baker, L.K., Krafft, G.A. and LaDu, M.J. (2002) Oligomeric and fibrillar species of amyloid-beta peptides differentially affect neuronal viability. *J. Biol. Chem.* **277**, 32046–32053 https://doi.org/10.1074/jbc.M201750200

59 Cohen, J. (1988) *Statistical Power Analysis for the Behavioral Sciences*, L. Erlbaum Associates, Hillsdale, NJ

60 Faul, F., Erdfelder, E., Buchner, A. and Lang, A.-G. (2009) Statistical power analyses using G*Power 3.1: Tests for correlation and regression analyses. *Behav. Res. Methods* **41**, 1149–1160 https://doi.org/10.3758/BRM.41.4.1149

61 Wong, N. and Wang, X. (2015) miRDB: an online resource for microRNA target prediction and functional annotations. *Nucleic Acids Res.* **43**, D146–D152 https://doi.org/10.1093/nar/gku1104

62 Fishilevich, S., Nudel, R., Rappaport, N., Hadar, R., Plaschkes, I., Iny Stein, T., et al. (2017) Genehancer: genome-wide integration of enhancers and target genes in geneCards. *Database* **2017**, bax028 https://doi.org/10.1093/database/bax028

63 Hallberg, B. and Palmer, R.H. (2013) Mechanistic insight into ALK receptor tyrosine kinase in human cancer biology. *Nat. Rev. Cancer* **13**, 685–700 https://doi.org/10.1038/nrc3580

64 van Amerongen, R., Mikels, A. and Nusse, R. (2008) Alternative wnt signaling is initiated by distinct receptors. *Sci. Signal.* **1**, re9 https://doi.org/10.1126/scisignal.135re9

65 Palomer, E., Buechler, J. and Salinas, P.C. (2019) Wnt signaling deregulation in the aging and Alzheimer's brain. *Front. Cell. Neurosci.* **13**, 227 https://doi.org/10.3389/fncel.2019.00227

66 Krützfeldt, J. and Stoffel, M. (2010) Regulation of wingless-type MMTV integration site family (WNT) signalling in pancreatic islets from wild-type and obese mice. *Diabetologia* **53**, 123–127 https://doi.org/10.1007/s00125-009-1578-2

67 Chen, J., Ning, C., Mu, J., Li, D., Ma, Y. and Meng, X. (2021) Role of Wnt signaling pathways in type 2 diabetes mellitus. *Mol. Cell. Biochem.* **476**, 2219–2232 https://doi.org/10.1007/s11010-021-04086-5

68 Jensen, K.P. and Covault, J. (2011) Human miR-1271 is a miR-96 paralog with distinct non-conserved brain expression pattern. *Nucleic Acids Res.* **39**, 701–711 https://doi.org/10.1093/nar/gkq798

69 Kong, D., Zhang, G., Ma, H. and Jiang, G. (2015) miR-1271 inhibits OSCC cell growth and metastasis by targeting ALK. *Neoplasma* **62**, 559–566 https://doi.org/10.4149/neo_2015_067

70 Cai, T., Long, J., Wang, H., Liu, W. and Zhang, Y. (2017) Identification and characterization of miR-96, a potential biomarker of NSCLC, through bioinformatic analysis. *Oncol. Rep.* **38**, 1213–1223 https://doi.org/10.3892/or.2017.5754

71 Sani, M.R.M., Hashemzadeh-Chaleshtori, M., Saidijam, M., Jami, M.-S. and Ghasemi-Dehkordi, P. (2016) MicroRNA-183 family in inner ear: hair cell development and deafness. *J. Audiol. Otol.* **20**, 131–138 https://doi.org/10.7874/jao.2016.20.3.131

72 Zhang, H., Zhang, S., Zhang, J., Liu, D., Wei, J., Fang, W. et al. (2018) ZO-1 expression is suppressed by GM-CSF via miR-96/ERG in brain microvascular endothelial cells. *J. Cereb. Blood Flow Metab.* **38**, 809–822 https://doi.org/10.1177/0271678X17702668

73 Kim, Y.C. and Guan, K.-L. (2015) mTOR: a pharmacologic target for autophagy regulation. *J. Clin. Invest.* **125**, 25–32 https://doi.org/10.1172/JCI73939

74 Jung, C.H., Ro, S.-H., Cao, J., Otto, N.M. and Kim, D.-H. (2010) mTOR regulation of autophagy. *FEBS Lett.* **584**, 1287–1295 https://doi.org/10.1016/j.febslet.2010.01.017

75 Russell, R.C., Yuan, H.-X. and Guan, K.-L. (2014) Autophagy regulation by nutrient signaling. *Cell Res.* **24**, 42–57 https://doi.org/10.1038/cr.2013.166

76 Spilman, P., Podlutskaya, N., Hart, M.J., Debnath, J., Gorostiza, O., Bredesen, D. et al. (2010) Inhibition of mTOR by rapamycin abolishes cognitive deficits and reduces amyloid-β levels in a mouse model of Alzheimer's disease. *PLoS ONE* **5**, e9979 https://doi.org/10.1371/journal.pone.0009979

77 Ost, A., Svensson, K., Ruishalme, I., Brännmark, C., Franck, N., Krook, H. et al. (2010) Attenuated mTOR signaling and enhanced autophagy in adipocytes from obese patients with type 2 diabetes. *Mol. Med. Camb. Mass* **16**, 235–246 https://doi.org/10.2119/molmed.2010.00023

78 Chen, X.-F., Zhang, Y., Xu, H. and Bu, G. (2013) Transcriptional regulation and its misregulation in Alzheimer's disease. *Mol. Brain* **6**, 44 https://doi.org/10.1186/1756-6606-6-44

79 Villa, C., Ridolfi, E., Fenoglio, C., Ghezzi, L., Vimercati, R., Clerici, F., et al. (2013) Expression of the transcription factor Sp1 and its regulatory hsa-miR-29b in peripheral blood mononuclear cells from patients with Alzheimer's disease. *J. Alzheimers Dis.* **35**, 487–494 https://doi.org/10.3233/JAD-122263

80 Kulyté, A., Belarbi, Y., Lorente-Cebrián, S., Bambace, C., Arner, E., Daub, C.O. et al. (2014) Additive effects of microRNAs and transcription factors on CCL2 production in human white adipose tissue. *Diabetes* **63**, 1248–1258 https://doi.org/10.2337/db13-0702

81 Chen, J., Meng, Y., Zhou, J., Zhuo, M., Ling, F., Zhang, Y. et al. (2013) Identifying candidate genes for type 2 diabetes mellitus and obesity through gene expression profiling in multiple tissues or cells. *J. Diabetes Res.* **2013**, e970435 https://doi.org/10.1155/2013/970435

82 Katso, R.M., Russell, R.B. and Ganesan, T.S. (1999) Functional analysis of H-Ryk, an atypical member of the receptor tyrosine kinase family. *Mol. Cell. Biol.* **19**, 6427–6440 https://doi.org/10.1128/MCB.19.9.6427

83 Bolognin, S., Lorenzetto, E., Diana, G. and Buffelli, M. (2014) The potential role of rho GTPases in Alzheimer's disease pathogenesis. *Mol. Neurobiol.* **50**, 406–422 https://doi.org/10.1007/s12035-014-8637-5

84 Jeanteur, P. (2012) *Cytoskeleton and Small G Proteins*, Springer Science & Business Media

85 Spiering, D. and Hodgson, L. (2011) Dynamics of the Rho-family small GTPases in actin regulation and motility. *Cell Adhes. Migr.* **5**, 170–180 https://doi.org/10.4161/cam.5.2.14403

86 Huang, T.Y., DerMardirossian, C. and Bokoch, G.M. (2006) Cofilin phosphatases and regulation of actin dynamics. *Curr. Opin. Cell Biol.* **18**, 26–31 https://doi.org/10.1016/j.ceb.2005.11.005

87 Minamide, L.S., Striegl, A.M., Boyle, J.A., Meberg, P.J. and Bamburg, J.R. (2000) Neurodegenerative stimuli induce persistent ADF/cofilin-actin rods that disrupt distal neurite function. *Nat. Cell Biol.* **2**, 628–636 https://doi.org/10.1038/35023579

88 Hernandes, M.S. and Britto, L.R.G. (2012) NADPH oxidase and neurodegeneration. *Curr. Neuropharmacol.* **10**, 321–327 https://doi.org/10.2174/157015912804499483

89 Brun, T. and Gauthier, B.R. (2008) A focus on the role of Pax4 in mature pancreatic islet beta-cell expansion and survival in health and disease. *J. Mol. Endocrinol.* **40**, 37–45 https://doi.org/10.1677/JME-07-0134

90 Mauvais-Jarvis, F., Smith, S.B., Le May, C., Leal, S.M., Gautier, J.-F., Molokhia, M., et al. (2004) PAX4 gene variations predispose to ketosis-prone diabetes. *Hum. Mol. Genet.* **13**, 3151–3159 https://doi.org/10.1093/hmg/ddh341

91 Nazarians-Armavil, A., Menchella, J.A. and Belsham, D.D. (2013) Cellular insulin resistance disrupts leptin-mediated control of neuronal signaling and transcription. *Mol. Endocrinol.* **27**, 990–1003 https://doi.org/10.1210/me.2012-1338

92 Kozieł, R., Pircher, H., Kratochwil, M., Lener, B., Hermann, M., Dencher, N.A. et al. (2013) Mitochondrial respiratory chain complex I is inactivated by NADPH oxidase Nox4. *Biochem. J.* **452**, 231–239 https://doi.org/10.1042/BJ20121778

93 Wang, X., Wang, W., Li, L., Perry, G., Lee, H. and Zhu, X. (2014) Oxidative stress and mitochondrial dysfunction in Alzheimer's disease. *Biochim. Biophys. Acta* **1842**, 1240–1247 https://doi.org/10.1016/j.bbadis.2013.10.015

94 Coletta, D.K. and Mandarino, L.J. (2011) Mitochondrial dysfunction and insulin resistance from the outside in: extracellular matrix, the cytoskeleton, and mitochondria. *Am. J. Physiol. Endocrinol. Metab.* **301**, E749–E755 https://doi.org/10.1152/ajpendo.00363.2011

95 Bedard, K. and Krause, K.-H. (2007) The NOX family of ROS-generating NADPH oxidases: physiology and pathophysiology. *Physiol. Rev.* **87**, 245–313 https://doi.org/10.1152/physrev.00044.2005

96 Meng, D., Lv, D.-D. and Fang, J. (2008) Insulin-like growth factor-I induces reactive oxygen species production and cell migration through Nox4 and Rac1 in vascular smooth muscle cells. *Cardiovasc. Res.* **80**, 299–308 https://doi.org/10.1093/cvr/cvn173

97 Gupta, A. and Dey, C.S. (2012) PTEN, a widely known negative regulator of insulin/PI3K signaling, positively regulates neuronal insulin resistance. *Mol. Biol. Cell* **23**, 3882–3898 https://doi.org/10.1091/mbc.e12-05-0337

98 Auer, M., Hausott, B. and Klimaschewski, L. (2011) Rho GTPases as regulators of morphological neuroplasticity. *Ann. Anat.* **193**, 259–266 https://doi.org/10.1016/j.aanat.2011.02.015

99 Lin, T., Zeng, L., Liu, Y., DeFea, K., Schwartz, M.A., Chien, S. et al. (2003) Rho-ROCK-LIMK-cofilin pathway regulates shear stress activation of sterol regulatory element binding proteins. *Circ. Res.* **92**, 1296–1304 https://doi.org/10.1161/01.RES.0000078780.65824.8B